Journal of Paleolithic Archaeology (2023) 6:6
https://doi.org/10.1007/s41982-022-00131-x

Pointing to the Ahmarian. Lithic Technology and the El-Wad Points of Al-Ansab 1

Jacopo Gennai[1] · **Marcel Schemmel**[1] · **Jürgen Richter**[1]

Accepted: 15 November 2022 / Published online: 3 January 2023

Abstract

The Ahmarian is the earliest fully fledged Upper Palaeolithic Levantine industry, and its hallmark is the el-Wad point, assumed to be a projectile implement. The Ahmarian is a blade-bladelet volumetric industry; however, bladelet production has frequently been portrayed as undifferentiated or secondary to blade production. El-Wad points are blades or bladelets with a fine to steep lateral retouch, often further shaping the tip. The role of bladelets and blades, both in the retouched and unretouched assemblages, is highly debated in order to refine Early Upper Palaeolithic (EUP) taxonomical and technological issues. Here, we use data coming from our excavations at the southern Ahmarian site of Al-Ansab 1 to reconsider the role of bladelets and el-Wad points in the assemblage. We show that bladelet production was key, and blades were mostly used to shape the convexities to produce convergent bladelets. El-Wad point blanks mostly stemmed from an early stage of the reduction sequence, being conventionally classified as small blades or big bladelets. Modification of these blanks likely improved their suboptimal shape, while smaller bladelets were not modified. Our detailed review of the existing literature produced corresponding evidence regarding lithic technology, while the exact function of el-Wad points is still pending on complementary use-wear analyses. With our new data, we expect to provoke a reconsideration of the Ahmarian technological system. As bladelets attract more and more attention in EUP research, we propose that the southern Ahmarian had already fully completed the technological and cultural shift to the preferred use of small projectile inserts.

Keywords Early Upper Palaeolithic · Levant · Chaîne opératoire · Typology · Bladelet · Ahmarian

Jacopo Gennai and Marcel Schemmel contributed equally to this work.

✉ Jacopo Gennai
jacopo.gennai@hotmail.it

✉ Marcel Schemmel
mschemm1@smail.uni-koeln.de

Extended author information available on the last page of the article

Introduction

The Early Ahmarian (hereafter Ahmarian) is the earliest fully fledged Upper Palaeolithic industry in the Levant (Belfer-Cohen & Goring-Morris, 2009; Gilead, 1991; Goring-Morris & Belfer-Cohen, 2018) (Fig. 1). It is associated with *H. sapiens* remains (Bergman & Stringer, 1989). Despite this status, the Ahmarian was one of the last taxonomical entities to be defined in Levantine prehistory, being conceived after surveys of the arid Sinai and Negev areas (Bar-Yosef & Belfer-Cohen, 1977; Gilead, 1981). The term Ahmarian was introduced earlier to name the Phases II–III assemblages of Erq el Ahmar, characterised by backed points (Font-Yves points) on blades and bladelets, and it was eventually used to describe the new assemblages found in the desert (Garrod, 1957; Gilead, 1981; Neuville, 1934). Hence, the Ahmarian came to define Levantine industries that are dominated by laminar technology and blade/bladelet tools, as opposed to the Levantine Aurignacian, which is

Fig. 1 The main Ahmarian sites in the Levant: (1) Abu Noshra I, II, IV; (2) Al-Ansab 1; (3) Boker A; (4) Kebara; (5) Ksar Akil; (6) Lagama V, VI, VII, VIII, XI, XII, XV, XVI; (7) Manot; (8) Mughr el-Hamamah; (9) Nahal Nizzana XIII; (10) Qadesh Barnea 501, 601, 602, 9; (11) Qafzeh; (12) Tor Hamar (J431); (13) Tor Sadaf; (14) Yabroud II; (15) Üçağızlı. Digital Elevation Model and bathymetry 1:10 m cross blended hypso with relief, water, drains, and ocean bottom (Naturalearthdata.com). EPSG: 4326, Map produced with QGIS 3.16 Hannover

dominated by burins and endscrapers (Gilead, 1981). Today, the Ahmarian refers to assemblages featuring narrow-fronted cores for the production of serial blades/bladelets, which are subsequently retouched into el-Wad points (slender and convergent blade/lets with partial or continuous marginal lateral retouch (Goring-Morris & Belfer-Cohen, 2018). When an Ahmarian industry is found stratified in multi-layered sites, it is preceded by the Initial Upper Palaeolithic and followed by the Levantine Aurignacian (e.g. Kebara cave, (Bar-Yosef & Belfer-Cohen, 2019); Ksar Akil, (Douka et al., 2013); Manot cave, (Abulafia et al., 2021); Tor Sadaf, (Fox, 2003); Üçağızlı, (Kuhn, 2004)).

In recent years, interest in the Ahmarian has been renewed by comparisons to the Protoaurignacian and the suggestion it could represent the first stage of *H. sapiens* dispersal into Europe (Hublin, 2015; Kadowaki et al., 2015; Teyssandier et al., 2010). Such a hypothesis relies mostly on dating, in addition to techno-typology similarities. Advocates of a direct relationship between the Ahmarian and the European record depend on the early radiometric determinations obtained in Kebara, Manot and Ksar Akil, where the start of the Ahmarian is placed between 46 and 43 ka cal BP (Alex et al., 2017; Bosch et al., 2015; Rebollo et al., 2011). However, critics point to the risk of charcoal contamination due to postdepositional processes (Zilhão, 2013) and the much younger determinations obtained for Ksar Akil and Üçağızlı (Douka, 2013; Douka et al., 2013, 2015; Kuhn et al., 2009). Single-layered open-air contexts, such as those often found in the Negev and Sinai, are more in line with a younger determination, even though some of these dates could represent minimal values (Gilead, 1991; Richter et al., 2020). The southern Ahmarian is dated as early as ca. 42 ka cal BP, roughly contemporaneous with the European Early Upper Palaeolithic (EUP; Boaretto et al., 2021; Phillips, 1994; Weinstein, 1984).

As the definition of the Ahmarian is a broadly laminar volumetric industry characterised by el-Wad points, its range was expanded to assemblages in the central and northern Levant, although assemblages in these areas show a different technological system. The northern Ahmarian is mostly characterised by opposed-platforms prismatic blade cores, although rare single-platform bladelet cores are also present (Abulafia et al., 2021; Bar-Yosef & Belfer-Cohen, 2019; Kuhn et al., 2009; Ohnuma, 1988; Tostevin, 2013). The southern Ahmarian is instead characterised by single-platform narrow-fronted cores producing contemporaneously slender, straight and convergent blades and bladelets (for instance Bar-Yosef & Belfer-Cohen, 1977; Coinman, 2003; Davidzon & Goring-Morris, 2003; Goring-Morris & Belfer-Cohen, 2018; Monigal, 2003). These blades and bladelets can be modified into el-Wad points by lateral marginal retouch and have become the fossil directeur of the Ahmarian (Goring-Morris & Belfer-Cohen, 2018; Le Brun-Ricalens et al., 2009; Marks, 1976).

In the first half of the twentieth century, Bate and Garrod gave the earliest accounts of retouched points in what would become the Ahmarian, relating the type to the Font-Yves point commonly associated with the European EUP (Garrod, 1957; Le Brun-Ricalens et al., 2009). At the London Symposium in 1969, it was decided to rename them el-Wad points: the term stood for curved and twisted small blade and bladelet blanks with a retouched distal tip and some additional retouch along the edge (Bar-Yosef & Belfer-Cohen, 1977; Le Brun-Ricalens

et al., 2009). Later, Marks would define the el-Wad point as 'a small blade or bladelet pointed by fine obverse retouch' (Marks, 1976, p. 381). While the stress eventually returned to direct retouch (Bergman, 1981; Shea, 2013), over the years there was a proliferation of subtypes describing some subtle differences in the extent and location of the retouched part (Ksar Akil points (Bergman, 1981); Abu Halka points (Bergman, 1981)) and the *pointe à face plane* in Ksar Akil, a leaf-shaped point with invasive retouch (Bergman, 1988). Since this typological variability hampers meaningful comparisons, an attempt to provide a standard operative categorisation according to the morphology of the blank and the location and type of retouch was proposed by Le Brun-Ricalens and colleagues (Le Brun-Ricalens et al., 2009). Also worth considering is the morphometric variability of el-Wad points. An analysis of Lagama VII, a site with a large number of el-Wad points, suggested that el-Wad points are a distinct group among the Ahmarian retouched blades and bladelets, especially considering the typometry of the blanks (50–55 mm long and 8–10 mm wide (Bar-Yosef & Belfer-Cohen, 1977)). Kadowaki and colleagues showed a significant difference in length and in the length/width ratio between el-Wad points respectively associated with southern and northern Ahmarian sites, with the northern Ahmarian points being longer and wider than their southern counterparts (Kadowaki et al., 2015). This could be related to the mostly blade-oriented knapping in northern Ahmarian sites. Nevertheless, there is a morphological similarity between el-Wad points and other marginally retouched blades and bladelets in Ahmarian contexts (e.g. Bar-Yosef & Belfer-Cohen, 1977; Monigal, 2003, Fig. 11.9). As implied by the name 'point', el-Wad points are assumed to be projectile tips or implements in a projectile shaft (e.g. Yaroshevich et al., 2021). Some studies devoted to the recognition of impact fractures on el-Wad points are available but lack conclusive results (Bergman, 1981; Coinman, 2005; Newcomer & Bergman, 1983).

The role of bladelets in Ahmarian contexts, even though highlighted typologically in the earliest publications (Bar-Yosef & Belfer-Cohen, 1977; Gilead, 1981), has been progressively subsumed in the blade production, with a rather unspecific and secondary role (Davidzon & Goring-Morris, 2003; Monigal, 2003; Phillips, 1988). The Protoaurignacian, frequently compared with the Ahmarian, followed a similar path: once considered an industry typologically composed of bladelets (Laplace, 1966) to a view of the lamellar component as mostly a result of to the final exploitation of former blade cores or to unspecific blade/bladelet production (Bon, 2002). Recently, various authors have stated the bladelet-based nature of the Protoaurignacian technological system (Bataille et al., 2018; Falcucci et al., 2020). Therefore, a reanalysis of the Ahmarian is needed to understand if EUP industries are bladelet based or if this innovation occurred earlier in Europe than in the Levant. Furthermore, the el-Wad point has become a problematic cultural marker because of how loosely it is used in various contexts. Through the technological and typological analyses of the Al-Ansab 1 AH1 assemblage, therefore, we seek to define the role of bladelet knapping and the place of el-Wad points in the Ahmarian technological system.

Materials and Methods

Al-Ansab 1 (hereafter Ansab) is located in the Lower Wadi Sabra (30°14′2.4″N 35°22′58.8″E; 618 m above sea level (a.s.l.); Fig. 1) in remnant Pleistocene sediments protected from erosion by a limestone ridge (Richter et al., 2020). Geoarchaeological analyses show that the sediments are sands and gravels originating from fluvial and aeolian deposits. At the time of the Ahmarian occupation, the bed of the wadi, now ca. 20 m below the archaeological site, was level with archaeology-bearing sediments, which corresponds well with a general level of aggradation during Marine Isotope Stage 3 (Bertrams et al., 2012). Optically stimulated luminescence dating has confirmed that rapid aggradation occurred between 45 and 32 ka (Bertrams et al., 2012; Klasen et al., 2013).

Because of the proximity to the wadi, the archaeological horizon was frequently flooded, but this did not alter nor re-orient the distribution of finds and anthropogenic structures (Bertrams et al., 2012; Schoenenberg & Sauer, 2022). In the course of seven excavation campaigns (2009–2020), two archaeological layers have been found, separated by consolidated sands. Only the topmost layer AH1 has been fully investigated (Richter et al., 2020; Schoenenberg & Sauer, 2022; Fig. 2). Charcoal recovered in the AH1 and further down in the section, corresponding to AH2, shows that the site was occupied during a brief span between 38 and 37 ka cal BP (Table 1; Richter et al., 2020; Schoenenberg & Sauer, 2022). So far, a 56.5-m^2 surface has been excavated, and a wider scatter of eroded artefacts was found on the slope. In fact, at the moment of the discovery two erosional steps with artefacts were present—it was only later that an upper find layer and a lower find layer were determined as the two in-situ sources of artefacts found to be mixed around the lower erosional step (Richter et al., 2020; Schoenenberg & Sauer, 2022).

Extending to the north of the upper erosional step lays the bulk of the Ahmarian occupation surface, which is rich in lithic finds (over 50,000 artefacts excluding

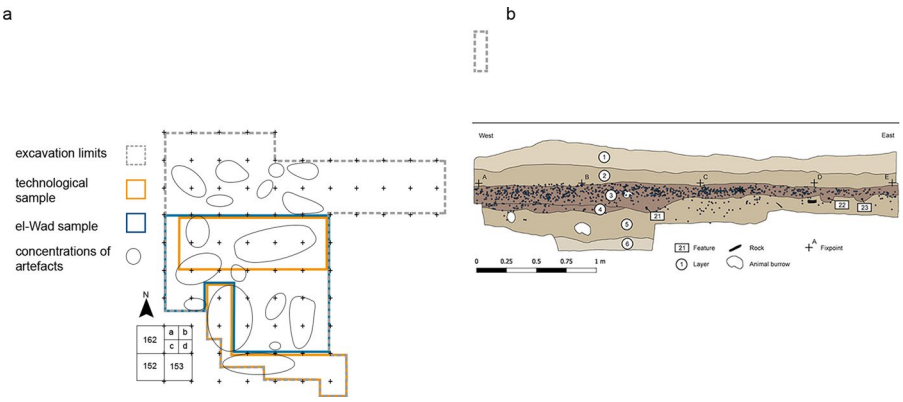

Fig. 2 **a** Grid plan of the excavated area (square units progress from left to right, tens from bottom to top), main artefact concentrations (redrawn from Parow-Souchon et al., 2021; Schoenenberg & Sauer, 2022) and the area sampled for the technological and the el-Wad points analyses. **b** Ansab section profile, squares 185–188 (Richter et al., 2020)

Table 1 Radiometric dates of Al-Ansab 1 (Richter et al., 2020)

ID number	Location	Material	Conv. age	±	Age cal. 1σ (68.3%)	Age cal. 2σ (95.4%)
AN001	AH1 N-S Trench	Charcoal	32,869	409	38,100–36,710	38,955–36,402
AN002	AH1, sq. 168	Charcoal	33,041	419	38,415–36,975	39,125–36,597
AN003	AH1, sq. 184a	Charcoal	33,292	432	38,875–37,430	39,312–36,897
AN004	AH2, N-S Trench	Charcoal	33,564	444	39,119–37,743	39,534–37,107
AN005	AH2, N-S Trench	Charcoal	33,552	460	39,117–37,715	39,555–37,070
AN006	AH2, N-S Trench	Charcoal	32,937	439	38,310–36,826	39,064–36,451
AN007	AH2, N-S Trench	Charcoal	33,447	440	39,020–37,630	39,420–37,019

Calibration was conducted using the Intcal20 calibration curve (Reimer et al., 2020) provided by the OxCal 4.4 software package (Bronk Ramsey, 2009)

chips) associated with charcoal, ochre and some faunal remains (mostly gazelle, *Gazella* sp.) and marine shell fragments (Cardiidae family) (Richter et al., 2020; Sauer & Schoenenberg, 2021; Schoenenberg & Sauer, 2022; Fig. 2). The richness in lithic artefacts is attributed to the nearby availability of good-quality cherts. Indeed, Ansab would have been a location where whole groups repeatedly visited in their quests for food, water and raw material resources (Parow-Souchon, 2020; Parow-Souchon et al., 2021; Sauer & Schoenenberg, 2021; Schyle, 2015). Raw material for AH1 lithics comes from the good quality Umm Rijam Chert Limestone (URC) and Al-Hisa Phosphorite/Amman Silicified Limestone (AHP/ASL) formations. Parow-Souchon performed detailed macroscopical and microscopical determinations of raw material on an assemblage (N 2466) made of all classes of debitage (Parow-Souchon, 2020; Parow-Souchon et al., 2021). The vast majority of the studied assemblage is fashioned on raw material acquired near the site (40–500 m), while a few pieces ($N=43$) come from a 12–18-km distance (Parow-Souchon et al., 2021). Nevertheless, this exotic raw material does not account for specialised use or class of artefact (Parow-Souchon et al., 2021). The recognised artefacts scatter does not show any variance in composition, leading to the deduction that human groups performed unspecific activities in a regime of residential mobility (Parow-Souchon, 2020; Richter et al., 2020; Schoenenberg & Sauer, 2022). The site is excavated using a 1-m^2 basic grid unit, which is further subdivided into quadrants of 0.25 m^2. Layers are geological and are excavated in arbitrary 5-cm-deep spits. Finds ≥ 10 mm in maximum dimension have been individually piece-plotted using a total station since 2015. Finds > 20 mm have two or more points plotted to record the contour. Smaller finds are identified by quadrant and spit number alongside finds retrieved by dry sieving through a 2-mm mesh.

Artefacts here presented come solely from AH1. The technological analysis study sample consists of single plotted complete and semi-complete blanks and cores recovered during the 2009–2011 and 2018 campaigns (Table 2). Hence, the technological sample derives from already studied material (2009–2011) (Hussain, 2015; Parow-Souchon et al., 2021; Schyle, 2015) and unpublished material (2018). The technological analysis sample consists of artefacts from squares 156, 157, 158, 164, 165, 166, 167, 168, 174, 184 (2009–2011) and squares 193, 194, 195, 196, 197, 198,

Table 2 Study sample divided per technical category and fragmentation

	Blade	Bladelet	Flake	Cores	El-Wad	Total
Complete	530	311	270	125	25	1261
Prox + Mes	179	303	13			495
Mes + Dist	238	195	11			444
Total	947	809	294			2200

203, 204, 205, 206, 207, 208 (2018; Fig. 2). The analysed artefacts cover different concentrations, but since the composition of these is even and raw material use and procurement are homogeneous, the sample is deemed representative for techno-typological purposes. The sample for the typological analysis consists of complete ($n = 12$) and nearly complete ($n = 13$) el-Wad points from 2015, 2017 and 2018 campaigns (Fig. 2).

As nearly complete artefacts still allow a valid estimation of the overall shape of the point, they are included with complete el-Wad points. Other retouched blades or bladelets were not taken into consideration, as only two complete artefacts are present. Although more el-Wad points might be present among the fragments, we decided to not include them because el-Wad points are defined to be pointed through retouch, and therefore completeness and the evaluation of the whole modified edge are chiefly important. Here, we preferred to use the Shea definition: 'el-Wad points are pointed blades or bladelets whose tips are shaped by fine and/or steep retouch, usually on their dorsal face. The amount of retouch along one or both lateral edges varies widely, as does the location of this retouch on dorsal or ventral faces' (Shea, 2013, p. 140). Nevertheless, some morphological blank attributes (outline, symmetry, profile) according to Le Brun-Ricalens and colleagues (Le Brun-Ricalens et al., 2009) were also taken into consideration. A blank is defined as semi-complete when it features at least a portion of the mesial part in addition to the distal or the proximal end. Blades and bladelets are defined as blanks with sub-parallel edges which are roughly twice as long as they are wide when complete (Andrefsky, 2005; Inizan et al. 1999). An arbitrary threshold of 12 mm width is applied for differentiating blades from bladelets (Tixier, 1963). Cores are defined as artefacts whose last blow did not produce a ventral face and show at least three negatives (Conard et al., 2004; Soressi & Geneste, 2011).

The technological analysis has been performed according the *chaîne opératoire* approach (Audouze & Karlin, 2017; Inizan et al. 1999; Schlanger, 2004; Soressi & Geneste, 2011). Cores and debitage have been closely inspected to retrieve the diacritical diagram (the arrangement of negatives revealing the goal of the knapping sequence (Inizan et al. 1999, p. 126)) and allow the reconstruction of the knapping stages (mental refitting). Later, each artefact was analysed to record its discrete attributes (Table 3).

After these considerations, artefacts have been classified as initialisation (removing cortex, opening cores), management (opening and renewing convexities), simple (flattening convexities), tablets (opening and renewing core striking platforms) and burin spalls (the result of burin blow technique (Inizan et al.

Table 3 Attributes used in the technological analysis

Attribute	Recorded On	Meaning	Reference	Notes
Proximal part				
Cores blank	Cores	Proxy of raw material use		Blank (it has a ventral flaked face), cobble (rounded shape and abraded cortex), nodule (fresh cortex), slab (squat tabular shape), squared chunk (undeterminable squared piece)
Knapping angle (*angle de chasse*)	Cores and blanks	Proxy of technique	(Inizan et al. 1999; Pelegrin, 2011)	< 70° (really acute), 70–90° (moderately acute), ≥ 90°
Lipping	Blanks	Proxy of technique	(Pelegrin, 2011)	
Bulb morphology	Blanks	Proxy of hammer type and technique	(Pelegrin, 2000)	Pronounced, bulbar scar, diffuse
Platform morphology	Cores and blanks	Proxy of technique	(Andrefsky, 2005; Scerri et al., 2016)	
Striking platform relationship	Cores	Proxy of main knapping direction		Number of striking platforms and position on the core volume
Whole blank				
Cores blank	Cores	Proxy of raw material use		Blank (it has a ventral flaked face), cobble (rounded shape and abraded cortex), nodule (fresh cortex), slab (squat tabular shape), squared chunk (undeterminable squared piece)
Negatives' orientation	Cores and blanks	Proxy of main knapping direction	(Scerri et al., 2016)	
Negatives' type	Cores and blanks	Proxy of the main production		Last negative with a whole measurable width

Table 3 (continued)

Attribute	Recorded On	Meaning	Reference	Notes
Cortex coverage	Blanks	Proxy of reduction depth and location on core volume	Modified from Andrefsky (2005)	Non-cortical (0–1%), semi-cortical (≥1 ≤50%), extensively cortical (≥51 ≤90%), entames (≥91%)
Cortex position	Cores and blanks	Proxy of location on core volume		According to the flaking direction
Overhang removal	Cores and laminar/lamellar blanks	Proxy of technique	(Pelegrin, 2011)	
Longitudinal profile	Laminar/lamellar blanks	Proxy of distal reach of the artefacts	(Bon, 2002; Scerri et al., 2016)	Straight, slightly curved, curved, very curved, twisted
Mid-cross section shape	Laminar/lamellar blanks	Proxy of blank location on the core volume	(Scerri et al., 2016)	Triangular, trapezoidal
Mid-cross section symmetry	Laminar/lamellar blanks	Proxy of blank location on the core volume	(Falcucci et al., 2017)	Symmetrical, asymmetrical
Distal termination	Laminar/lamellar blanks	Proxy of distal reach of the artefacts	(Andrefsky, 2005; Scerri et al., 2016)	Feathered, plunged, stepped, hinged
Outlines	Laminar/lamellar blanks	Proxy of flaking surface shape and location on the core volume	(Scerri et al., 2016)	Subparallel edges, convergent, off-axis

1999)). The management blanks consist of sub-categories such as crests shaping an artificial or natural pre-existing ridge, asymmetrical blanks laterally struck at the edges of flaking surfaces, overshot blanks removing the distal part of the core, maintenance blanks generically related to shaping purposes and surface cleaning blanks which show a high amount of previous negatives clearing the flaking surface for the next full debitage episode. Cores have been classified following the flaking surface morphology: pre-core (abandoned at the early shaping stage), parallel edges (broad surface framed by parallel edges (Bon, 2002)), semi-tournant (semi-circumferential flaking surface involving adjacent faces (Bon, 2002; Falcucci & Peresani, 2018)), narrow fronted (narrow flaking surface isolated through flank negatives (Davidzon & Goring-Morris, 2003; Falcucci & Peresani, 2018)), narrow-fronted sur tranche (natural narrow surface (Normand & Turq, 2005)), transversal carinated (broad flaking surface on a front slicing the artefact's thickness (Bon, 2002; Chiotti & Cretin, 2011)) and non-organised cores. Similar artefact measurements have been taken for both technological and typological samples. The length is measured according to the knapping axis on complete blanks. The width and thickness are measured at approximately mid-artefact length. Curvature is derived from the measurement of the distance from a plain surface (Fléche) at mid-length of complete blanks lying on their ventral surface following the formula $\frac{Fléche \times 100}{Length}$ and the values proposed in Bon (2002). Knapping angles are measured with an analogue protractor. The investigation of retouch follows the methodology and terminology of Inizan and colleagues (Inizan et al. 1999, p. 87). The retouch location of el-Wad points was mapped by dividing the artefact into six even zones for each ventral and dorsal face (Fig. 3).

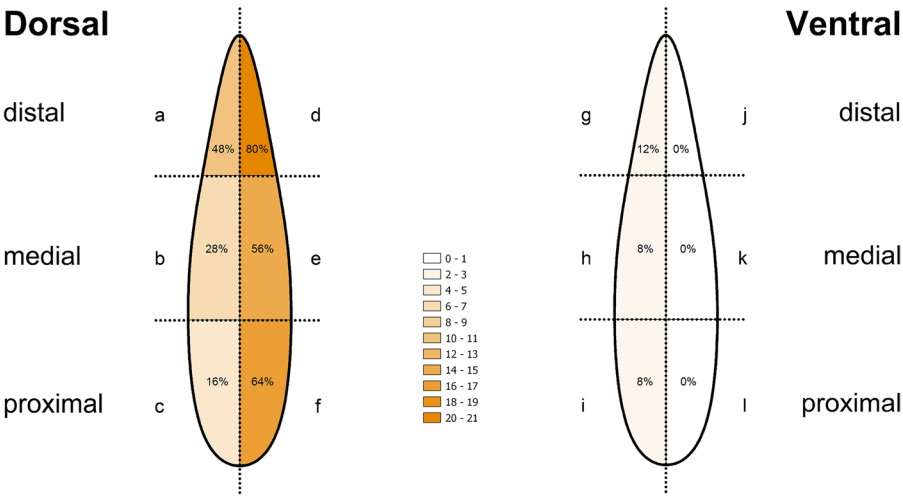

Fig. 3 Partition of the artefact for retouch recording

Results

Results are presented separately for technological and typological analysis. An interpretative combination will be provided in the discussion.

Result of the Technological Analysis

Cores

Only platform cores are present. Most of the cores are either semi-tournant or narrow-fronted (Table 4). Dimensionally, they can be grouped into broader cores (semi-tournant, parallel edges and transversal carination) and narrower cores (narrow fronted and sur tranche) (Table 5; Figs. 4 and 5). The Mann–Whitney test between two independent groups found a statistical similarity between the semi-tournant and the parallel edge cores' elongation ($W = 132.50$, $p = 0.422$, $r = -0.17$, $CI_{95\%}$ $[-0.52, 0.23]$, $n_{obs} = 40$). On the other hand, sur tranche cores are significantly more elongated than narrow-fronted cores ($W = 121.00$, $p < 0.001$, $r = -0.61$, $CI_{95\%}$ $[-0.78, -0.36]$, $n_{obs} = 55$). Semi-tournant and narrow-fronted cores are statistically different ($W = 270.50$, $p < 0.001$, $r = -0.52$, $CI_{95\%}$ $[-0.70, -0.29]$, $n_{obs} = 68$). Despite this, the morphological and dimensional difference is very fluid and, as later illustrated, the cores probably derive from a similar reduction method (Fig. 5).

Nearly half of the cores (46%; Table 6: cores' blank) are far too reduced to determine the original raw material form. While cobbles and nodules are preferred for semi-tournant, narrow-fronted and parallel edge cores, former flakes are common for sur tranche examples (73%; Table 6: core blanks). Cores management operations give a consistent picture of the whole sample. Knapping angles are acute, < 70° (74%; Table 6: flaking angle). Only sur tranche cores show a sizeable share of less acute angles, 70–90° (38%; Table 6: flaking angle). The overhang is regularly micro-chipped (89%; Table 6: overhang abrasion). Only sur tranche cores show a significant frequency of non-chipped cores (25%; Table 6: overhang abrasion). Cortex is generally present in faces not involved in the main flaking surface, thus mostly the posterior faces are left untouched (combined 57%; Table 6: cortex). Cores that do not involve lateral faces in the main flaking surface (parallel edges, narrow fronted) are more likely to have a lateral cortical face (Table 6: cortex). Striking platforms are kept plain (95%; Table 6: striking platform type) and cores mostly have a single platform (86%; Table 6: striking platform relationship). Negatives are determined from measurements of the last complete negatives; most of the cores produce

Table 4 Cores categories, the other category groups include fragmented ($N = 5$), blades and flake non-organised cores ($N = 5$) and ND ($N = 1$)

Pre-core		Parallel edges		Semi-tournant		Narrow fronted		Sur tranche		Trans. carinated		Other		Total	
N	%	*N*	%	*N*	%	*N*	%	*N*	%	*N*	%	*N*	%	*N*	%
7	6	11	9	34	27	41	33	16	13	5	4	11	9	125	100

Table 5 Summary of cores metrics, only complete cores are included

	Pre-core	Parallel edges	Semi-tournant	Narrow fronted	Sur tranche	Trans. carinated	Other
Length							
Count	7	11	29	39	16	5	4
MIN	43.3	28.4	27.0	26.2	20.2	20.3	25.0
IQ	52.6	34.4	35.7	42.6	42.2	24.7	34.8
Med	68.0	44.0	46.8	53.3	53.0	31.0	40.9
IIIQ	90.7	50.2	52.6	63.1	60.5	37.0	47.9
MAX	124.5	79.0	86.0	96.0	82.9	56.0	60.0
Width							
Count	7	11	29	39	16	5	4
MIN	28.8	26.8	20.0	17.2	7.2	35.7	27.7
IQ	36.7	35.8	32.5	28.0	17.0	45.0	44.8
Med	41.6	42.8	40.0	35.9	25.2	46.2	53.3
IIIQ	60.7	44.5	45.3	38.5	32.0	76.0	58.3
MAX	89.1	53.0	53.0	51.1	48.0	85.0	65.0
Thickness							
Count	7	11	29	39	16	5	4
MIN	43.3	28.4	27.0	26.2	20.2	20.3	25.0
IQ	52.6	34.4	35.7	42.6	42.2	24.7	34.8
Med	68.0	44.0	46.8	53.3	53.0	31.0	40.9
IIIQ	90.7	50.2	52.6	63.1	60.5	37.0	47.9
MAX	124.5	79.0	86.0	96.0	82.9	56.0	60.0
Elongation							
Count	7	11	29	39	16	5	4
MIN	0.9	0.7	0.7	0.6	1.0	0.5	0.5
IQ	1.2	1.0	1.1	1.3	1.8	0.5	0.5
Med	1.4	1.1	1.2	1.5	2.0	0.6	0.9
IIIQ	2.0	1.4	1.4	1.8	2.7	0.7	1.3
MAX	2.6	1.5	1.9	3.2	4.5	0.7	1.6

bladelets (30%; Table 6: negative types) or a combination of bladelets and blades (38%; Table 6: negative types). Only a few (14%; Table 6: negative types) are abandoned with mostly blade negatives. The negative orientation is largely unidirectional (73%; Table 6: negative directions) followed by unidirectional and convergent (19%; Table 6: negative directions).

Debitage

Blades and bladelets account for the vast majority of the debitage in the assemblage (Fig. 6). More than half of the blades and flakes are management blanks, while bladelets are mostly simple blanks (Table 7). Flakes are also prevalent in

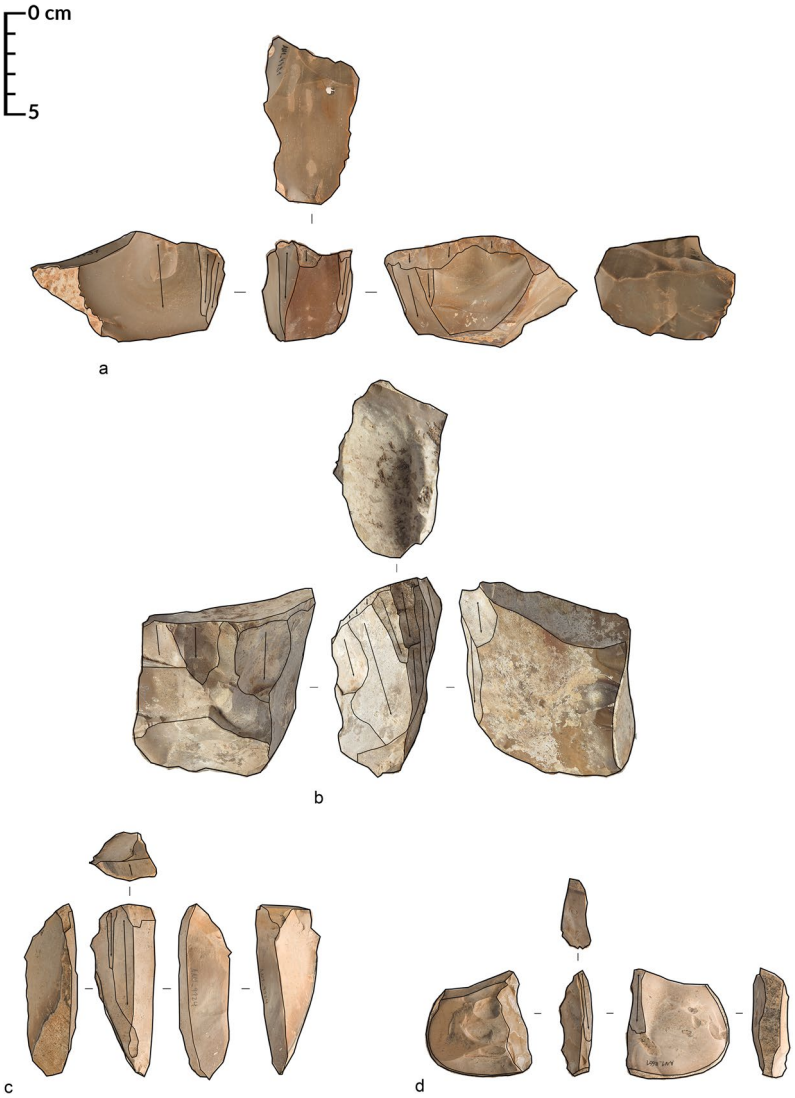

Fig. 4 Narrow cores. **a**, **b** Abandoned at an early stage; **c**, **d** sur tranche cores. (**b**) Shows that bladelets, central last negatives, were the sought-after blanks. (**a**) Shows that the core front was left cortical and instead multiple single flaking surfaces were initially exploited around lateral ridges (photos: J. Gennai)

initialisation and tablets (Table 7). Within management blanks, asymmetrical ones are the most frequent in blades (47%; Table 7) and bladelets (70%; Table 7), while surface cleaning is the most frequent category in flakes (88%; Table 7).

The majority of the assemblage is non-lipped (59%; Table 8: lipping). Lipping occurs mostly in blades (57%; Table 8: lipping) and flakes (58%; Table 8: lipping), while it is negligible in bladelets (16%; Table 8: lipping). Blades and

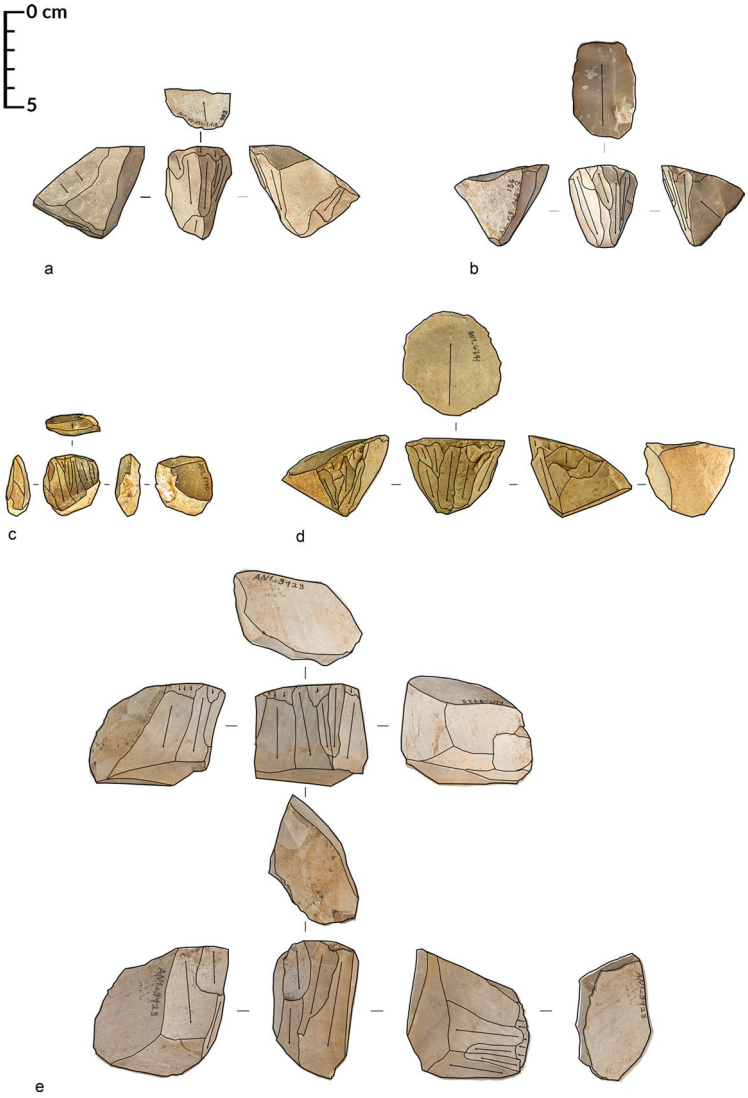

Fig. 5 Broad (**c**, **d**), narrow (**b**) and multiple flaking surfaces (broad and narrow) cores (**a**, **e**). The goal of the knapping is unchanged regardless of the extent of the flaking surface: bladelets are obtained from central areas framed by bigger negatives (photos: J. Gennai)

bladelets have mostly diffuse bulbs (Table 8: bulb). Flakes have either diffuse (43%; Table 8: bulb) or pronounced bulbs (41%; Table 8: bulb), diffuse bulbs being more common in management and simple blanks. Flakes have also a higher percentage of bulbar scars (12%; Table 8: bulb). Overhang removal is highly frequent among blades and bladelets (81%; Table 8: overhang abrasion). Knapping angles are mostly acute, 70–90° (44%; Table 8: flaking angle) followed by very

Table 6 Cores' attributes

	Pre-core		Parallel edges		Semi-tournant		Narrow fronted		Sur tranche		Trans. carinated		Other		Total	
	N	%	*N*	%	*N*	%	*N*	%	*N*	%	*N*	%	*N*	%	*N*	%
OVERHANG ABRASION																
Yes	5	71	11	100	33	97	40	98	12	75	5	100	5	45	111	89
No	2	29			1	3	1	2	4	25			6	55	14	11
Total	7	100	11	100	34	100	41	100	16	100	5	100	11	100	125	100
FLAKING ANGLE																
< 70°	2	29	9	82	28	82	34	83	9	56	4	80	6	55	92	74
70–90°	3	43	2	18	3	9	7	17	6	38	1	20	1	9	23	18
> 90°	1	14													1	1
Indeterminate	1	14			3	9			1	6			4	36	9	7
Total	7	100	11	100	34	100	41	100	16	100	5	100	11	100	125	100
CORES BLANK																
Determinate	6	86	7	64	15	44	22	54	11	69	3	60	4	36	68	54
Blank	3	50					1	5	8	73	2	67	1	25	15	22
Cobble	1	17	3	43	9	60	11	50					2	50	26	38
Nodule	2	33	3	43	3	20	7	32	1	9	1	33	1	25	18	26
Slab							1	5	2	18					3	4
Squared chunk			1	14	3	20	2	9							6	9
Indeterminate	1	14	4	36	19	56	19	46	5	31	2	40	7	64	57	46
Total	7	100	11	100	34	100	41	100	16	100	5	100	11	100	125	100
CORTEX																
With cortex	5	71	11	100	22	65	31	76	9	56	1	20	5	45	84	67
Lateral	2	40	4	36	1	5	5	16	3	33			2	40	17	20
Back			3	27	10	45	10	32					1	20	24	29
Back and base			2	18	5	23	4	13	1	11					12	14

Table 6 (continued)

	Pre-core		Parallel edges		Semi-tournant		Narrow fronted		Sur tranche		Trans. carinated		Other		Total	
	N	%	*N*	%	*N*	%	*N*	%	*N*	%	*N*	%	*N*	%	*N*	%
Back and lateral			1	9	3	14	6	19	2	22					12	14
Base	1	20	1	9	2	9	5	16	1	11			1	20	11	13
Other	2	40			1	5	1	3	2	22	1	100	1	20	8	10
No cortex	2	29			12	35	10	24	7	44	4	80	6	55	41	33
Total	7	100	11	100	34	100	41	100	16	100	5	100	11	100	125	100
STRIKING PLATFORM TYPE																
Natural					1	3	3	7							4	3
Plain	7	100	11	100	33	97	38	93	16	100	5	100	9	82	119	95
Indeterminate													2	18	2	2
Total	7	100	11	100	34	100	41	100	16	100	5	100	11	100	125	100
STRIKING PLATFORM RELATIONSHIP																
Single	6	86	9	82	29	85	36	88	16	100	4	80	8	73	108	86
Opposed	1	14	1	9	3	9	1	2					1	9	7	6
Opposed auxiliary							1	2							1	1
Adjacent							1	2			1	20			2	2
Independent			1	9	1	3	2	5					1	9	5	4
Orthogonal auxiliary					1	3									1	1
Indeterminate									0				1	9	1	1
Total	7	100	11	100	34	100	41	100	16	100	5	100	11	100	125	100
NEGATIVES' TYPES																
Bladelets			3	27	12	35	14	34	6	38	1	20	2	18	38	30
Blades and bladelets	2	29	4	36	14	41	18	44	8	50	1	20	1	9	48	38

Table 6 (continued)

	Pre-core		Parallel edges		Semi-tournant		Narrow fronted		Sur tranche		Trans. carinated		Other		Total	
	N	%	*N*	%	*N*	%	*N*	%	*N*	%	*N*	%	*N*	%	*N*	%
Blades	1	14	2	18	3	9	7	17	1	6	1	20	3	27	18	14
Bladelets and flakes			2	18	1	3							1	9	4	3
Blades and flakes	1	14			1	3			1	6	1	20			4	3
Blades, bladelets and flakes					3	9	2	5							5	4
Flakes	2	29									1	20	4	36	7	6
No negatives	1	14													1	1
Total	7	100	11	100	34	100	41	100	16	100	5	100	11	100	125	100
NEGATIVES' DIRECTION																
Bidirectional			1	9	2	6			2	13			1	9	6	5
Convergent													1	9	1	1
Unidirectional	5	71	10	91	25	74	28	68	11	69	4	80	8	73	91	73
Unidirectional + convergent	1	14			6	18	12	29	3	19	1	20	1	9	24	19
Unidirectional variants					1	3	1	2							2	2
No negatives	1	14													1	1
Total	7	100	11	100	34	100	41	100	16	100	5	100	11	100	125	100

The Other category groups include fragmented ($N=5$), blades and flake non-organised cores ($N=5$) and ND ($N=1$)

Fig. 6 Blade and bladelet debitage. **a–c** Crests, **d–h** asymmetrical blades, **i–l** overshot blades, **m–r** simple blades, **s–x** simple bladelets, **z** burin spall (photos: J. Gennai)

acute, < 70° (37%; Table 8: flaking angle). Blades have a higher frequency of very acute angles (45%; Table 8: flaking angle). Plain, linear and punctiform platforms account for almost the whole debitage assemblage (Table 8: platforms). Linear and punctiform platforms are most typical of blades and bladelets, linear being equally frequent in blades (43%; Table 8: platforms) and bladelets (45%; Table 8: platforms), while punctiform increases in bladelets (29% against 17% of blades;

Table 7 Blanks' categories

	Blade		Bladelet		Flake	
	N	%	*N*	%	*N*	%
Initialisation					53	18
Management	503	53	110	14	162	55
Asymmetrical	237	47	77	70		
Crest	72	14	7	6		
Overshot	141	28	19	17		
Maintenance	18	4	7	6	20	12
Surface cleaning	35	7			142	88
Tablet	1	< 1			48	16
Simple	442	47	688	85	29	10
Spall			10	1		
Total	946		808		292	

Table 8: platforms). Faceted platforms are common only in core tablets (35%; Table 8: platforms).

The number of cortex-bearing artefacts falls from flakes (47%; Table 9: cortex) to blades (29%; Table 9: cortex) to bladelets (6%; Table 9: cortex). Flakes are the only blanks having artefacts devoted entirely to the core decortication and have the highest frequency of entames (17%; Table 9: cortex) and artefacts with more than three-quarters of the dorsal face covered in the cortex (17%; Table 9: cortex). Semi-cortical debitage accounts for the most frequent cortical artefacts in the assemblage (82% of debitage with cortex; Table 9: cortex) and for nearly all the cortical blades and bladelets (89%; Table 9: cortex). A lateral position, according to the knapping direction, of the cortical area is most common in blades (51% of the semi-cortical artefacts; Table 9: cortex) and bladelets (54% of the semi-cortical debitage; Table 9: cortex). The distal position is also common in blades (34% of the semi-cortical debitage; Table 9: cortex) and bladelets (37%; Table 9: cortex). Semi-cortical flakes are mostly lateral (47%; Table 9: cortex) and dorsal (23%; Table 9: cortex). Bladelets account for the most frequently determined negatives in the assemblage (67%; Table 9: negative types). Other than on bladelets themselves, bladelet negatives are found on most of the blades (59%; Table 9: negative types) and some flakes (17%; Table 9: negative types). Artefacts bearing unidirectional negatives are the majority across the debitage (combined 82% of artefacts with negatives; Table 9: negative orientation), followed by those only bearing convergent negatives (8%; Table 9: negative orientation).

Bladelets are mostly straight in profile (56%; Table 10: profile) followed by twisted (20%; Table 10: profile) and slightly curved (17%; Table 10: profile). Blades are less straight (38%; Table 10: profile), similarly slightly curved (18%; Table 10: profile) and more twisted (26%; Table 10: profile) and curved (15%; Table 10: profile). Blade cross-sections are mostly asymmetrical (67%; Table 10: cross-section) and trapezoidal (61%; Table 10: cross-section). Bladelet cross-sections are split between symmetrical (47%; Table 10: cross-section) and asymmetrical (46%;

Table 8 Debitage proximal part attributes

	Blade						Total blade		Bladelet						Total bladelet		Flake								Total flake		Grand total	
	Simple		Mgmt		Tablet				Simple		Mgmt		Spall				Simple		Mgmt		Init		Tablet					
	N	%	*N*	%	*N*	%	*N*	%	*N*	%	*N*	%	*N*	%	*N*	%	*N*	%	*N*	%	*N*	%	*N*	%	*N*	%	*N*	%
LIPPING[a]																												
Yes	162	52	220	60			382	57	73	14	21	27	1	33	95	16	13	52	89	60	32	65	24	50	158	58	635	41
No	147	48	145	40	1	100	293	43	439	86	58	73	2	67	499	84	12	48	60	40	17	35	24	50	113	42	905	59
Total	309	100	365	100	1	100	675	100	512	100	79	100	3	100	594	100	25	100	149	100	49	100	48	100	271	100	1540	100
BULB[b]																												
Diffuse	251	79	284	73			535	76	426	81	66	80	2	33	494	80	16	59	77	49	15	31	14	29	122	43	1151	72
Not perceived	5	2	1	0			6	1	39	7	1	1	1	17	41	7											47	3
Pronounced	43	13	67	17	1	100	111	16	44	8	11	13			55	9	9	33	56	36	28	57	21	44	114	41	280	17
Bulbar scar	15	5	26	7			41	6	9	2	3	4			12	2	2	7	21	13	5	10	7	15	35	12	88	5
Crushed	2	1	7	2			9	1	3	1			2	33	5	1					1	2	3	6	4	1	18	1
ND	3	1	3	1			6	1	5	1	1	1	1	17	7	1			3	2			3	6	6	2	19	1
Total	319	100	388	100	1	100	708	100	526	100	82	100	6	100	614	100	27	100	157	100	49	100	48	100	281	100	1603	100
FLAKING ANGLE[a]																												
< 70°	124	40	180	49	1	100	305	45	145	28	28	35		0	173	29	8	32	62	42	18	37	8	17	96	35	574	37
70–90°	146	47	132	36			278	41	225	44	34	43	1	33	260	44	13	52	71	48	22	45	33	69	139	51	677	44
> 90°																			2	1			1	2	3	1	3	0
ND	39	13	53	15			92	14	142	28	17	22	2	67	161	27	4	16	14	9	9	18	6	13	33	12	286	19
Total	309	100	365	100	1	100	675	100	512	100	79	100	3	100	594	100	25	100	149	100	49	100	48	100	271	100	1540	100
OVERHANG ABRASION[a]																												
Yes	290	94	300	82			590	87	421	82	59	77	2	67	482	81											1072	85
No	19	6	67	18			86	13	91	18	18	23	1	33	110	19											196	15
Total	309	100	367	100			676	100	512	100	77	100	3	100	592	100											1268	100

Table 8 (continued)

	Blade						Total blade		Bladelet						Total bladelet		Flake								Total flake		Grand total	
	Simple		Mgmt		Tablet				Simple		Mgmt		Spall				Simple		Mgmt		Init		Tablet					
	N	%	*N*	%	*N*	%	*N*	%	*N*	%	*N*	%	*N*	%	*N*	%	*N*	%	*N*	%	*N*	%	*N*	%	*N*	%	*N*	%
PLATFORMS[b]																												
Plain	91	29	142	37	1	100	234	33	105	20	15	18	1	17	121	20	14	52	83	53	27	55	21	44	145	52	500	31
Linear	158	50	145	37			303	43	253	48	26	32			279	45	6	22	40	25	7	14	2	4	55	20	637	40
Puncti-form	57	18	64	16			121	17	138	26	38	46	2	33	178	29			7	4	4	8	1	2	12	4	311	19
Dihedral			2	1			2										1	4	4	3	1	2	2	4	8	3	10	1
Faceted																			2	1	1	2	17	35	20	7	20	1
Natural	2	1	8	2			10	1	4	1					4	1	1	4	10	6	5	10	1	2	17	6	31	2
ND	1	0	4	1			5	1	12	2					12	2	3	11	3	2	4	8	4	8	14	5	31	2
Crushed	10	3	23	6			33	5	14	3	3	4	3	50	20	3	2	7	8	5		0		0	10	4	63	4
Total	319	100	388	100	1	100	708	100	526	100	82	100	6	100	614	100	27	100	157	100	49	100	48	100	281	100	1603	100

Mgmt management, *Init* initialisation

[a]Complete and Prox + Mes without crushed platforms

[b]Complete and Prox + Mes

Table 9 Whole artefact debitage attributes

	Blade						Total blade		Bladelet						Total bladelet		Flake								Total flake		Grand total	
	Simple		Mgmt		Tablet				Simple		Mgmt		Spall				Simple		Mgmt		Init		Tablet					
	N	%	*N*	%	*N*	%	*N*	%	*N*	%	*N*	%	*N*	%	*N*	%	*N*	%	*N*	%	*N*	%	*N*	%	*N*	%	*N*	%
CORTEX[a]																												
No cortex	**393**	**89**	**281**	**56**			**674**	**71**	**671**	**98**	**81**	**74**	**10**	**100**	**762**	**94**	**21**	**72**	**104**	**64**			**30**	**63**	**155**	**53**	**1591**	**78**
With cortex	**49**	**11**	**222**	**44**	**1**	**100**	**272**	**29**	**17**	**2**	**29**	**26**			**46**	**6**	**8**	**28**	**58**	**36**	**53**	**100**	**18**	**38**	**137**	**47**	**455**	**22**
Semi-cortical	45	92	195	88	1	100	241	89	15	88	26	90			41	89	8	100	52	90	17	32	14	78	91	66	373	82
Lateral	29	64	93	48	1	100	123	51	9	60	13	50			22	54	4	50	28	54	3	18	8	57	43	47	188	50
Distal	9	20	74	38			83	34	3	20	12	46			15	37	2	25	11	21	5	29	1	7	19	21	117	31
Dorsal	7	16	20	10			27	11	1	7	1	4			2	5			9	17	8	47	4	29	21	23	50	13
Proximal			8	4			8	3	1	7					1	2	2	25	4	8	1	6	1	7	8	9	17	5
Proximal and distal									1	7					1	2											1	0
Extensively cortical	4	8	19	9			23	8	2	12	3	10			5	11			5	9	16	30	2	11	23	17	51	11
Lateral	2	50	6	32			8	35												0		0		0		0	8	16
Distal																			1	20		0		0	1	4	1	2
Dorsal	2	50	13	68			15	65	2	100	3	100			5	100			4	80	16	100	2	100	22	96	42	82
Entames			8	4			8	3											1	2	20	38	2	11	23	17	31	7
Distal			1	13			1	13																			1	3
Dorsal			7	88			7	88											1	100	20	100	2	100	23	100	30	97
Total	442	100	503	100	1	100	946	100	688	100	110	100	10	100	808	100	29	100	162	100	53	100	48	100	292	100	2046	100
NEGATIVES' TYPES[a]																												
Determinate negatives	319	72	401	80	1	100	721	76	392	57	82	75			474	59	6	21	101	62	18	34	39	81	164	56	1359	66
Bladelets	251	79	174	43			425	59	392	100	66	80			458	97			18	18	1	6	9	23	28	17	911	67

Table 9 (continued)

	Blade						Total blade		Bladelet						Total bladelet		Flake								Total flake		Grand total	
	Simple		Mgmt		Tablet				Simple		Mgmt		Spall				Simple		Mgmt		Init		Tablet					
	N	%	*N*	%	*N*	%	*N*	%	*N*	%	*N*	%	*N*	%	*N*	%	*N*	%	*N*	%	*N*	%	*N*	%	*N*	%	*N*	%
Bladelets and flakes	1	0	23	6			24	3			3	4			3	1			6	6			4	10	10	6	37	3
Blades	20	6	56	14			76	11			3	4			3	1			26	26			3	8	29	18	108	8
Blades and bladelets	46	14	97	24	1	100	144	20			7	9			7	1			11	11			7	18	18	11	169	12
Blades and flakes	1	0	12	3			13	2											5	5			3	8	8	5	21	2
Blades, bladelets and flakes			9	2			9	1													1	6	4	10	5	3	14	1
Flakes			30	7			30	4			3	4			3	1	6	100	35	35	16	89	9	23	66	40	99	7
Indeterminate	122	28	87	17			209	22	270	39	23	21	2	20	295	37	15	52	58	36	9	17	4	8	86	29	590	29
No negatives	1	0	15	3			16	2	26	4	5	5	8	80	39	5	8	28	3	2	26	49	5	10	42	14	97	5
Total	442	100	503	100	1	100	946	100	688	100	110	100	10	100	808	100	29	100	162	100	53	100	48	100	292	100	2046	100
NEGATIVES' ORIENTATION[a]																												
With negatives	441	100	488	97	1	100	930	98	662	96	105	95	2	20	769	95	21	72	159	98	27	51	43	90	250	86	1949	95
Bipolar	13	3	18	4	1	100	32	3	6	1	1	1			7	1	1	5	5	3	3	11			9	4	48	2
Bipolar variants	1	0	5	1			6	1	1	0		0			1	0					1	4	1	2	2	1	9	0
Convergent	30	7	48	10			78	8	63	10	9	9			72	9	1	5	10	6					11	4	161	8
Convergent variants			3	1			3	0				0															3	0

Table 9 (continued)

	Blade						Total blade		Bladelet						Total bladelet		Flake								Total flake		Grand total	
	Simple		Mgmt		Tablet				Simple		Mgmt		Spall				Simple		Mgmt		Init		Tablet					
	N	%	*N*	%	*N*	%	*N*	%	*N*	%	*N*	%	*N*	%	*N*	%	*N*	%	*N*	%	*N*	%	*N*	%	*N*	%	*N*	%
Crossed	10	2	21	4			31	3	9	1	4	4			13	2	4	19	14	9	5	19	2	5	25	10	69	4
Crossed variants			1	0			1	0				0														0	1	0
Orthogonal			17	3			17	2			1	1			1	0	1	5	5	3	2	7	24	56	32	13	50	3
Unipolar	316	72	269	55			585	63	397	60	64	61	2	100	463	60	11	52	110	69	14	52	8	19	143	57	1191	61
Unipolar+convergent	57	13	53	11			110	12	174	26	13	12			187	24			7	4					7	3	304	16
Unipolar variants	13	3	53	11			66	7	12	2	13	12			25	3	2	10	8	5	2	7	8	19	20	8	111	6
Indeterminate	1	0		0			1	0									1	5							1	0	2	0
No negatives	1	0	15	3			16	2	26	4	5	5	8	80	39	5	8	28	3	2	26	49	5	10	42	14	97	5
Total	442	100	503	100	1	100	946	100	688	100	110	100	10	100	808	100	29	100	162	100	53	100	48	100	292	100	2046	100

Mgmt management, *Init* initialisation. In the Cortex section bold entries represent the total number of artefacts and the frequency of non-cortical artefacts against cortical ones. Semi-cortical, Extensively cortical and Entames are showing the breakdown of cortical categories within the cortical artefacts. Italics are showing the breakdown of cortical positions in each cortical category (i.e. Semi cortical)

[a]Complete and semi-complete

Table 10 Blade and bladelet morphotechnological attributes

	Blade				Blade total		Bladelet						Bladelet total		Total	
	Simple		Mgmt				Simple		Mgmt		Spall					
	N	%	*N*	%	*N*	%	*N*	%	*N*	%	*N*	%	*N*	%	*N*	%
PROFILE[a]																
Straight	259	59	97	19	356	38	425	62	18	16	9	90	452	56	808	46
Slightly curved	88	20	78	16	166	18	118	17	18	16			136	17	302	17
Curved	42	10	96	19	138	15	16	2	16	15			32	4	170	10
Very curved	1	<1	36	7	37	4	1	<1	1	1			2	<1	39	2
Twisted	47	11	194	39	241	26	106	15	56	51	1	10	163	20	404	23
Indeterminate	5	1	2	<1	7	1	22	3	1	1			23	3	30	2
Total	442	100	503	100	945	100	688	100	110	100	10	100	808	100	1753	100
CROSS SECTION[a]																
Flat	6	1	30	6	36	4	38	6	5	5			43	5	79	5
Indeterminate			1	<1	1	<1	11	2	3	3			14	2	15	1
Symmetric	177	40	94	19	271	29	351	51	17	15	9	90	377	47	648	37
Asymmetric	259	59	378	75	637	67	288	42	85	77	1	10	374	46	1011	58
Total	442	100	503	100	945	100	688	100	110	100	10	100	808	100	1753	100
Trapezoidal	286	65	292	58	578	61	299	43	33	30	1	10	333	41	911	52
Triangular	150	34	180	36	330	35	340	49	69	63	9	90	418	52	748	43
Total	442	100	503	100	945	100	688	100	110	100	10	100	808	100	1753	100
DISTAL END[a]																
Feathered	240	78	100	22	340	44	357	88	18	21	10	100	385	77	725	57
Plunged	32	10	266	58	298	39	9	2	58	68			67	13	365	29
Hinged	13	4	25	5	38	5	18	4	2	2			20	4	58	5
Stepped	12	4	66	14	78	10	9	2	6	7			15	3	93	7
Indeterminate	12	4	2	<1	14	2	15	4	1	1			16	3	30	2

Table 10 (continued)

	Blade				Blade total		Bladelet						Bladelet total		Total	
	Simple		Mgmt				Simple		Mgmt		Spall					
	N	%	*N*	%	*N*	%	*N*	%	*N*	%	*N*	%	*N*	%	*N*	%
Total	309	100	459	100	768	100	408	100	85	100	10	100	503	100	1271	100
OUTLINE[a]																
(sub)Parallel edges	163	53	205	45	368	48	139	34	22	26	8	80	169	34	537	42
Convergent	100	32	52	11	152	20	207	51	11	13	2	20	220	44	372	29
Off-axis	43	14	200	44	243	32	58	14	51	60			109	22	352	28
Indeterminate	3	1	2	<1	5	1	4	1	1	1			5	1	10	1
Total	309	100	459	100	768	100	408	100	85	100	10	100	503	100	1271	100

Mgmt management

[a]Complete and Mes + Dist

Table 10: cross-section), and they are mostly triangular (52%; Table 10: cross-section). Distal terminations in blades are mostly feathered (44%; Table 10: distal terminations), followed by plunged (39%; Table 10: distal termination). Bladelet distal terminations are significantly more feathered (77%; Table 10: distal termination), followed by plunged (13%; Table 10: distal termination). Outlines in blades are mostly sub-parallel (48%; Table 10: outlines), followed by off-axis (32%; Table 10: outlines). Bladelet outlines are mostly convergent (44%; Table 10: outlines), followed by sub-parallel (33%; Table 10: outlines). Chi-squared independence tests performed on the morpho-technological attributes show a significant difference between blades and bladelets (Fig. 7).

Analysis of the El-Wad Retouch

Most el-Wad points are made on bladelets (66%). Many are characterised by a straight profile (72%) with the remaining bladelets being slightly curved (24%). One was broken, so the curvature could not be measured accurately.

There are 14 different retouch combinations present within the assemblage (Fig. 8). The position of the retouch is mostly dorsal (Table 11). Comparing frequencies in lateralisation, the right dorsal edge is more prominent (Fig. 8). This is the result of most artefacts being either retouched on both dorsal edges ($n=13$, Table 11) or just the right dorsal edge ($n=8$, Table 11). Retouch along the left dorsal edge is limited to a single el-Wad point. However, the only lateralisation present within inversely retouched points is on the left ($n=3$, Table 11). Concerning the extent of the retouch, 15 artefacts show retouch of at least a single whole edge; 13 of them on the right edge, which may or may not include additional retouch on parts of the left edge (Fig. 8).

Our observations show that the type of retouch can vary from fine to steep and may also, in some instances, change along the same edge (Fig. 9b–d). A continuous retouch with no changes in its angle or the amount of material that was being removed is less frequent. The inverse retouch seems to be limited to the smallest points in the assemblage—three of the five shortest points can be linked to such retouch (Fig. 9g). Furthermore, there are no specific retouch types or combinations that can be attributed to either bladelets or blades.

The only el-Wad subtype found in Al-Ansab 1 is the Ksar Akil point (Fig. 9c; Bergman, 1981). In fact, five el-Wad points are straight in profile, symmetrical, dorsally retouched and have the metrical dimensions of blades. Other variations of el-Wad points, such as Abu Halka or Ouchtata points, are not present within the assemblage.

The Dimensions of Retouched and Non-retouched Components

As the el-Wad points usually display characteristics akin to simple blades and bladelets, we performed a Mann–Whitney independent samples test to compare their metrics with those of simple blades, bladelets, and combined blades and bladelets (Table 12). Lengthwise, el-Wad point distribution is independent of those of blades,

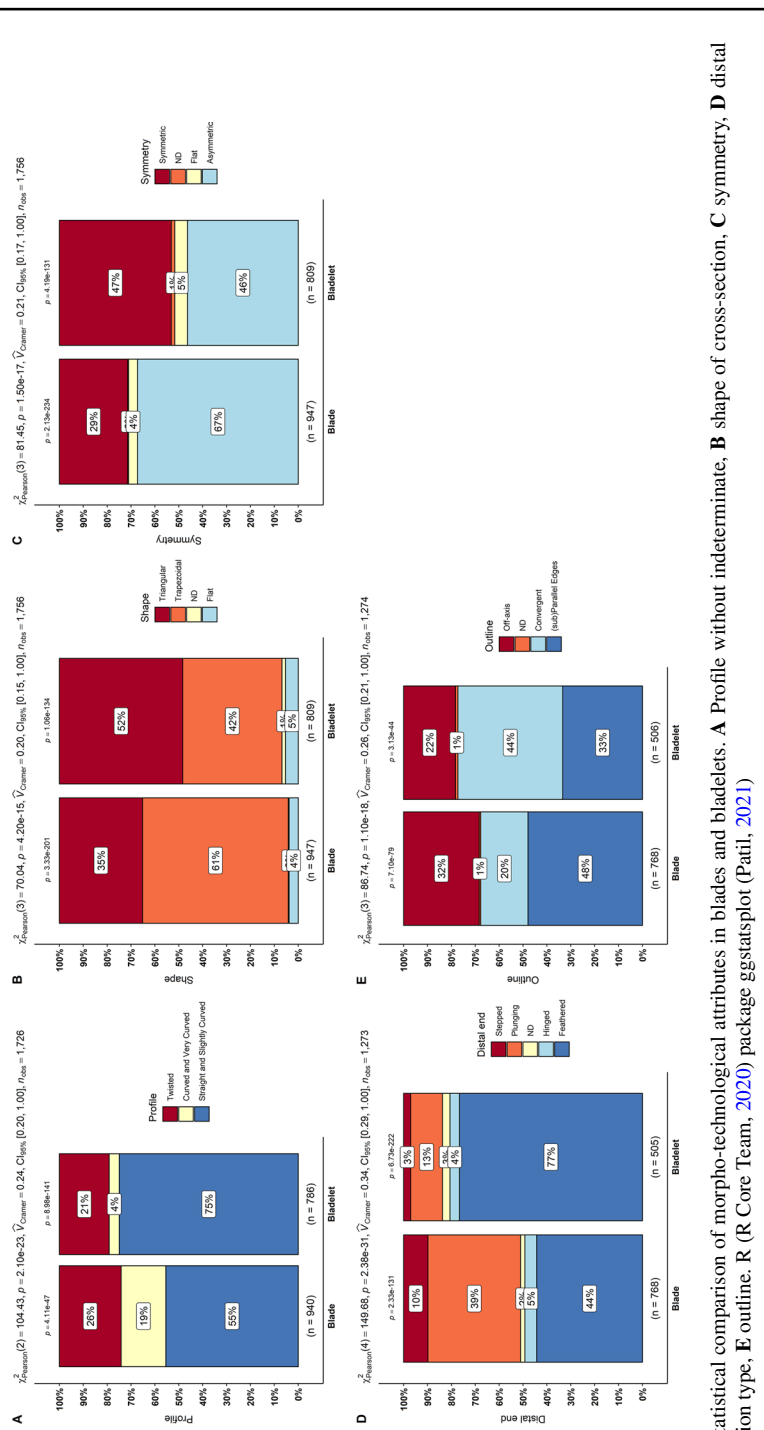

Fig. 7 Statistical comparison of morpho-technological attributes in blades and bladelets. **A** Profile without indeterminate, **B** shape of cross-section, **C** symmetry, **D** distal termination type, **E** outline. R (R Core Team, 2020) package ggstatsplot (Patil, 2021)

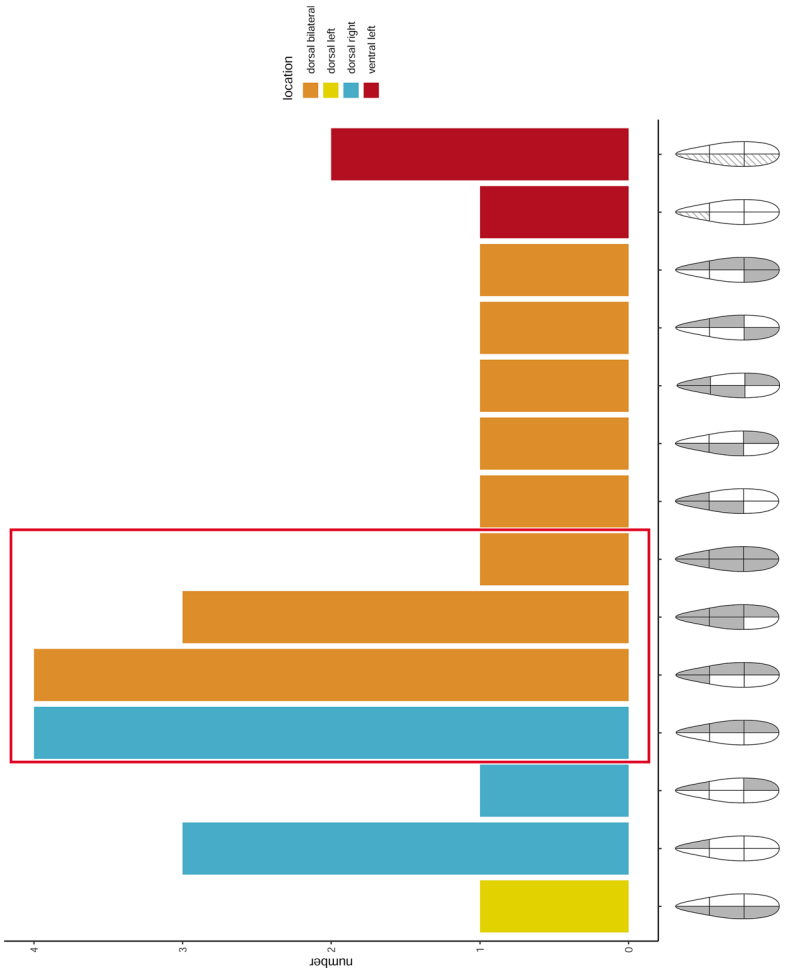

Fig. 8 Retouch combinations of dorsal and ventral retouched el-Wad points. The red box highlights points with a retouch along the entire right edge which can also have a retouch on the left lateral edge

Table 11 Retouch location on el-Wad points

	Localisation							
	Both		Left		Right		Total	
	N	%	*N*	%	*N*	%	*N*	%
Position								
Inverse	0	0	3	12	0	0	3	12
Direct	13	52	1	4	8	32	22	88
Total	13	52	4	16	8	32	25	100

bladelets, and blades and bladelets combined (Figs. 10A, 11A, and 12A). The width is independent of those of single blades and bladelets (Figs. 10B and 11B), but it statistically matches that of blades and bladelets combined (Fig. 12B). The thickness statistically matches that of the blades (Fig. 10C) but is statistically different from that of bladelets, and blades and bladelets combined (Figs. 11C and 12C). Similarly, el-Wad point curvature statistically matches that of the blades (Fig. 10D) but is different from bladelets, and blades and bladelets combined (Figs. 11D and 12D). The elongation of el-Wad points is statistically different from that of blades, bladelets, and blades and bladelets combined (Figs. 10E, 11E, and 12E).

Fig. 9 El-Wad points. **a**–**f**: El-Wad points with dorsal retouch combinations (c fits the Ksar Akil point type). **g**: Inversely retouched el-Wad point. **h**: distal el-Wad fragment with burination scar (highlighted in red) (photos M. Schemmel)

Table 12 Debitage metric summary

	Blade		Bladelet			El-Wad	Blade and bladelet			Flake				LCN Deb	LCN Core
	Simple	Mgmt	Simple	Mgmt	Spall		Simple	Mgmt	Spall	Simple	Mgmt	Tablet	Init		
Length															
N	186	344	245	57	6	25	431	401	6	25	151	46	46	226	60
MIN	23.7	25.0	10.0	18.0	29.0	26.6	10.0	18.0	29.0	20.2	20.0	19.2	21.7	9.0	13.0
IQ	38.4	46.9	22.6	30.0	33.1	45.8	26.9	44.0	33.1	32.2	38.7	41.6	35.5	20.0	22.1
Med	48.0	57.0	28.7	37.9	38.3	58.7	36.0	53.0	38.3	38.8	44.4	53.6	41.6	26.6	31.2
IIIQ	58.4	68.1	36.6	44.8	47.6	67.8	48.5	66.6	47.6	44.9	51.5	66.3	54.3	37.0	38.5
MAX	99.8	109.9	75.1	68.3	51.7	85.5	99.8	109.9	51.7	61.9	85.0	108.0	114.5	73.0	73.0
Width															
N	442	503	686	108	10	25	1128	611	10	29	162	48	53	938	108
MIN	12.0	12.0	3.0	5.1	2.9	6.5	3.0	5.1	2.9	19.8	17.0	8.4	21.9	2.0	3.0
IQ	13.2	15.7	7.0	8.2	4.3	10.2	8.0	13.0	4.3	28.4	27.2	28.9	32.4	4.9	7.2
Med	15.0	19.5	8.6	9.3	5.6	11.7	10.6	18.0	5.6	32.4	33.2	35.4	40.3	6.2	9.7
IIIQ	18.3	24.7	10.0	10.9	7.1	13.3	14.0	23.2	7.1	39.3	40.0	48.8	49.9	8.5	15.1
MAX	30.4	49.9	12.0	12.0	9.1	16.9	30.4	49.9	9.1	58.0	72.4	86.1	79.0	30.0	44.2
Thickness															
N	442	504	685	108	10	25	1127	612	10	29	162	48	53		
MIN	1.0	0.0	0.0	1.0	2.0	1.2	0.0	0.0	2.0	0.0	0.0	3.2	0.0		
IQ	3.0	4.9	1.8	2.9	3.5	2.8	2.0	4.0	3.5	3.8	5.3	7.9	6.7		
Med	4.0	6.1	2.0	3.0	5.4	3.4	3.0	5.8	5.4	4.9	7.0	12.2	9.0		
IIIQ	5.1	8.3	3.0	4.4	6.0	4.8	3.9	7.9	6.0	9.0	9.6	15.2	14.4		
MAX	11.3	43.0	5.7	10.0	8.3	5.7	11.3	43.0	8.3	15.8	36.2	30.0	31.3		
Elongation															
N	186	342	245	57	6	25	431	399	6	25	151	46	46	226	60
MIN	1.6	1.4	1.9	2.1	4.2	2.8	1.6	1.4	4.2	0.6	0.4	0.7	0.5	1.3	0.9

Table 12 (continued)

	Blade		Bladelet			El-Wad	Blade and bladelet			Flake				LCN Deb	LCN Core
	Simple	Mgmt	Simple	Mgmt	Spall		Simple	Mgmt	Spall	Simple	Mgmt	Tablet	Init		
IQ	2.5	2.2	2.8	3.4	5.3	4.2	2.6	2.3	5.3	0.9	1.1	0.9	0.9	3.7	2.3
Med	2.9	2.7	3.3	4.0	7.0	4.8	3.2	2.8	7.0	1.2	1.4	1.5	1.2	4.5	3.0
IIIQ	3.5	3.3	4.1	4.8	10.0	5.5	3.8	3.6	10.0	1.4	1.6	1.9	1.4	5.4	4.2
MAX	6.1	5.5	7.1	6.5	11.1	6.3	7.1	6.5	11.1	1.6	2.3	6.3	2.0	9.5	7.0
Curvature															
N	186	344	245	57	6	25									
MIN	0.0	0.0	0.0	0.0	0.0	0.1									
IQ	0.0	3.3	0.0	1.2	0.0	1.5									
Med	1.2	6.3	0.0	3.9	0.0	2.0									
IIIQ	4.0	8.5	2.9	5.4	0.0	2.9									
MAX	9.4	18.2	11.1	21.1	0.1	5.9									

Mgmt management, *Init* initialisation

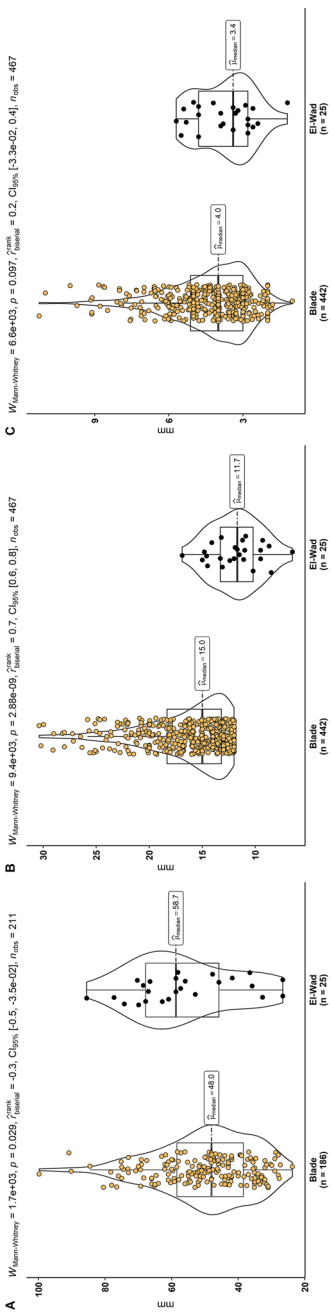

Fig. 10 Statistical comparison of metrical values of simple blades and el-Wad points. **A** Length, **B** width, **C** thickness, **D** curvature, **E** elongation. R (R Core Team, 2020) package ggstatsplot (Patil, 2021)

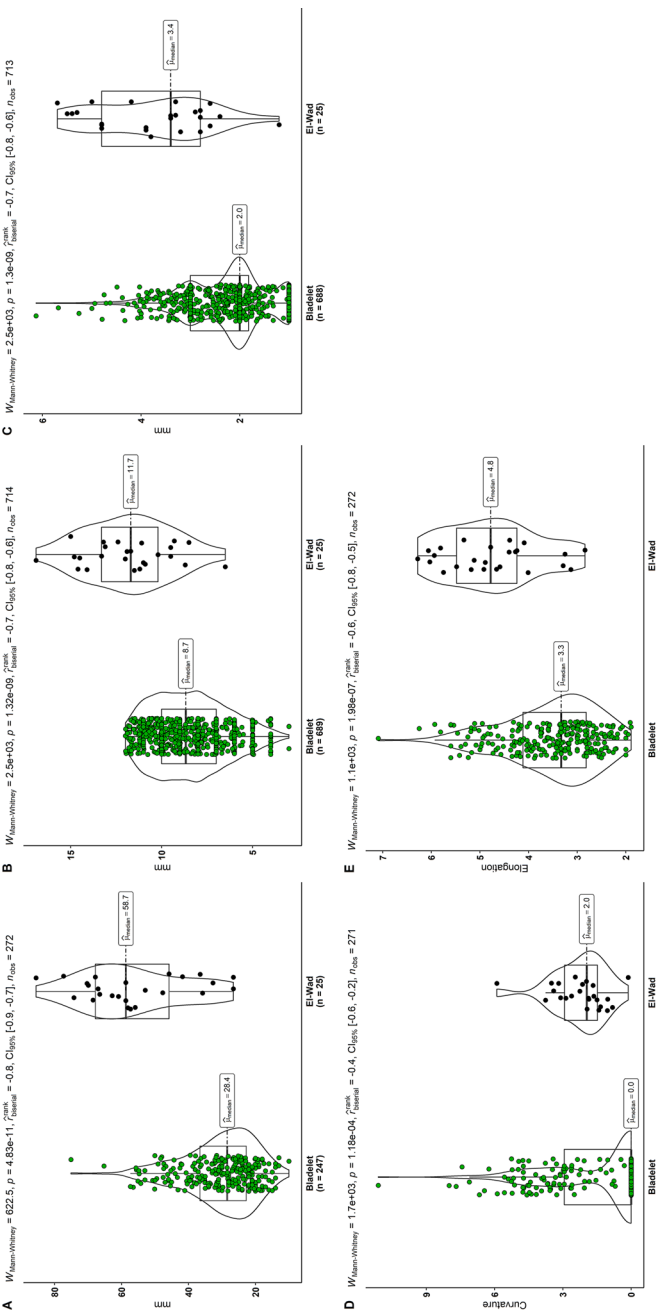

Fig. 11 Statistical comparison of metrical values of simple bladelets and el-Wad points. **A** Length, **B** width, **C** thickness, **D** curvature, **E** elongation. R (R Core Team, 2020) package ggstatsplot (Patil, 2021)

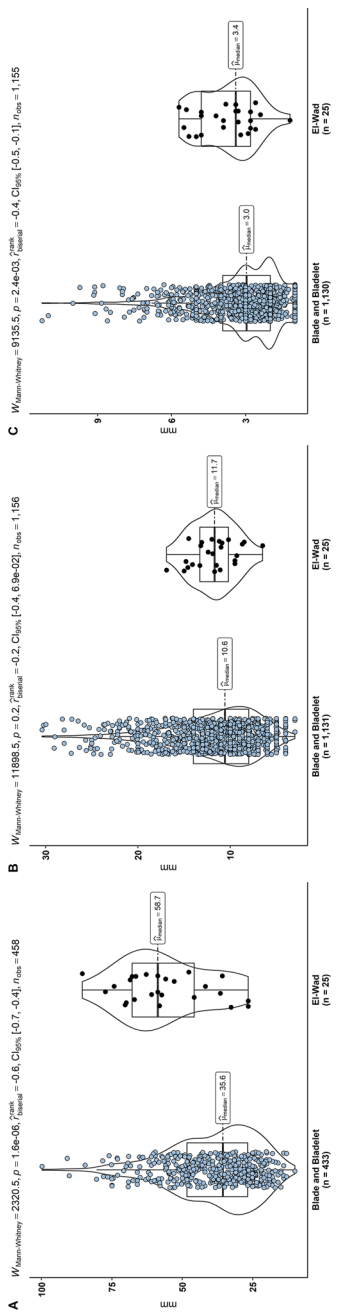

Fig. 12 Statistical comparison of metrical values of simple blades and bladelets and el-Wad points. **A** Length, **B** width, **C** thickness, **D** curvature, **E** elongation. R (R Core Team, 2020) package ggstatsplot (Patil, 2021)

Discussion

The technology and typology at Ansab have been previously assessed using the 2009–2011 material (Hussain, 2015; Parow-Souchon, 2020; Parow-Souchon et al., 2021; Schyle, 2015). While Schyle's (2015) and Hussain's (2015) work was mostly concerned with identifying Ahmarian techno-typological hallmarks, Parow-Souchon (2020; Parow-Souchon et al., 2021) is more concerned with integrating technology in the broader mobility system and with reconstructing raw material procurement. The present technological analysis built on these results and, focusing on bladelet technology, was included in the wider scope to assess technological conduits between the Ahmarian and the European EUP record (Gennai, 2021). Here, we limited ourselves to the comparisons between other Ahmarian assemblages. We enlarged the sample of the thoroughly studied AH1 lithics, adding artefacts retrieved during the 2018 excavation campaign.

Technology

The technological assessment is in fundamental agreement with Hussain (2015) and Parow-Souchon and colleagues (Parow-Souchon et al., 2021). Nevertheless, the interpretation has shifted, especially regarding the relationship between blades and bladelets.

The *chaine opératoire* is rather standardised and allows for almost no variation until the discard of the core (Fig. 13). It starts with collecting locally sourced, mostly tabular-shaped raw material (Parow-Souchon et al., 2021). The presence of a cortical surface on one of the lateral core faces and of a weathered surface on the back of the core is consistent with what was observed for cortex extent and position on cores and debitage. The preparation of the core striking platform and in general the decortication process uses flakes. Additional flakes are knapped during later operations of lateral adjustments of the flaking surface. Furthermore, flakes are the preferential blank class for the re-preparation of the striking platform along with the reduction.

The reduction follows a unidirectional mode. Only the tablets show an inversion of knapping direction since the core length is perpendicularly 'sliced' using the primary flaking surface as a striking platform. This results in seemingly faceted platforms, where the faceting corresponds to the former unidirectional negatives. Otherwise, the platforms are predominantly plain, linear or punctiform, supporting the plain striking platform observed on cores. The technical attributes (bulbs, flaking angle, overhang removal and platform morphology) generally support the notion of tangential, soft-hammer and direct percussion (Pelegrin, 2000, 2011). In particular, the previous Ansab analyses (Hussain, 2015; Parow-Souchon et al., 2021) suggested a differentiation of percussion techniques among blanks classes: hard-hammer, direct percussion for flakes and tangential, soft-hammer and direct percussion for blades. This is supported by the results reported here for bulbs, overhang and platforms, even though we urge caution in over-interpreting technical observations since experimental studies have shown that technical proxies could relate to other factors, such as the individual knapper's skill (Driscoll & García-Rojas, 2014; Roussel et al., 2009).

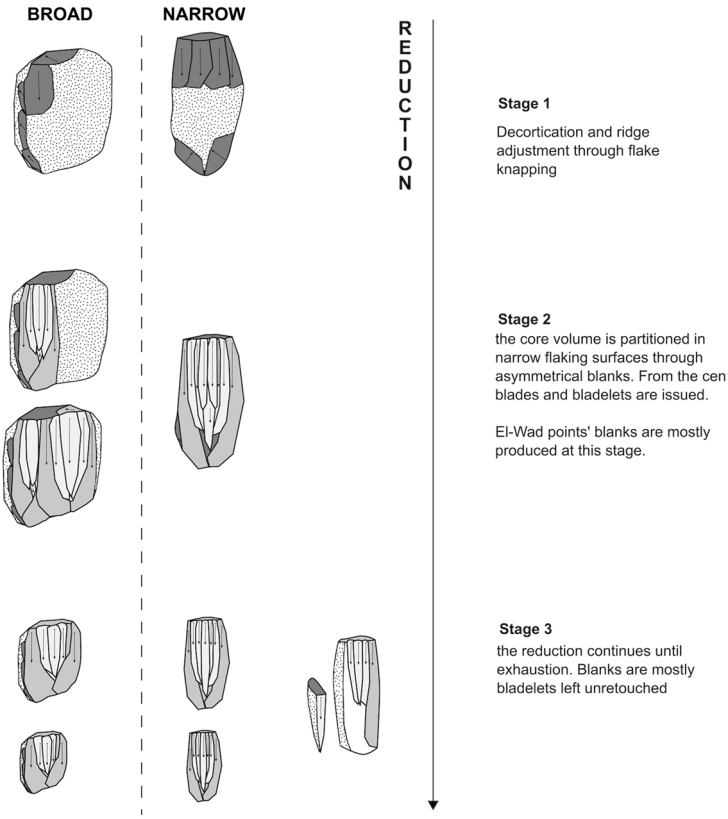

Fig. 13 Schematic rendition of the *chaîne opératoire* in Ansab. Dotted areas: cortical/natural, dark grey areas: former steps, light grey areas: actual reduction step. Figure produced with Inkscape 1.1

The initial convexity establishment seems primary to use naturally existing ridges, with minimal shaping. Therefore, crests are mostly unifacial. As evidenced also by Parow-Souchon and colleagues (Parow-Souchon et al., 2021), the flaking surface is decorticated in instalments, which leads to the interpretation that narrow flaking surfaces were subsequently exploited around ridges, shifting from one core side to another (Figs. 4 and 13). This is in accordance with the scarcity of fully cortical blades and bladelets. Another indication of the shifting of the flaking surface, at least until the core volume allows it, is the high frequency of asymmetrical management blades in the assemblage (Table 7). These blanks, already described in Hussain (2015) as *débordant* blades, are a way of shaping the distal and transversal convexities without major interruption of the simple debitage knapping. Due to their asymmetrical cross-section, plunged distal termination and twisted longitudinal profile, they are apt at encasing a flat, convergent volume exploited for simple debitage.

In the assemblage, the blanks that are consistent with the exploitation of these core volumes are mostly bladelets. There are multiple considerations to support this statement. First, the numbers: despite bladelets being less numerous than blades,

they are overwhelmingly classified as simple debitage (Table 7). Second, the type of negatives: most of them are bladelets in size and they occur on every blank class in the assemblage, regardless of size, therefore making it difficult to attribute these bladelets solely to advanced stages of the reduction or dedicated small cores. The frequency of indeterminate negatives in blanks is due to the incomplete width of many negatives since it is impossible to ascertain which category a negative belongs to without a metrical determination. Bladelet negatives may have an advantage in being represented due to their small dimensions making them detectable. On the other hand, finding bladelet negatives on larger elements, such as blades and flakes, shows that bladelets are not the implicit result of size reduction through knapping, but they are explicit knapping objectives. Third, the diacritic analysis: narrow core volumes call for narrow products. This is not exclusive to the southern Ahmarian but rather an occurrence diffused in other bladelet-based technologies (Bataille et al., 2018; Falcucci & Peresani, 2018; Falcucci et al., 2017; Gennai, 2021; Porraz et al., 2010; Slimak et al., 2002). Bladelet negatives are most often found in central positions, covering other negatives, and not exploiting the whole length of cores. This is consistent with their morpho-technological attributes showing a fundamentally straight, convergent morphology.

Some researchers working on Levantine assemblages prefer not to state a conceptual difference between blades and bladelets (cf. blade/lets Davidzon & Goring-Morris, 2003; blade(let)s Hussain, 2015, Schyle, 2015; blade/bladelets Monigal, 2003; target blades Parow-Souchon et al., 2021). Nevertheless, frequently Ahmarian assemblages are bladelet oriented if applying Tixier's threshold (1963). For example, in Nahal Nizzana XIII, where almost half of the material can be refitted, yielding important insights into the Ahmarian technical behaviour, most of the original nodules are flat and have flaking surfaces that rarely exceed 25 mm in width (Davidzon & Goring-Morris, 2003). Therefore, hardly any blade could be knapped from the central release surface. In Boker A, the combined blade and bladelet mean width is 12.3 mm, with the highest frequencies measured in the 7–11-mm interval (Monigal, 2003). In Ansab, the median length provided (31.5 mm) for Stage V blades is within the Tixier's bladelet length definition (Parow-Souchon et al., 2021). Despite this, Student *t*-tests comparing the length summary data of simple bladelets (mean = 30.6 mm, SD = 10.8) and simple blades and bladelets (mean = 38.8 mm, SD = 15.6) with their stage V blades (mean = 35.3 mm, SD = 16.4) show in both cases statistical independence between this sample and that of Parow-Souchon and colleagues ($p < 0.01$; $p < 0.01$). In the Jebel Qalkha area, the frequency of bladelets rises sharply during the Ahmarian, becoming the prevalent laminar blank (Kadowaki et al., 2021). In Tor Sadaf, bladelets by far outnumber the blades in the assemblage, and the mean width of the laminar debitage is 12.2 mm (Fox, 2003). Interest in producing bladelets can be deduced also from the Gebel Lagama sites (Bar-Yosef & Belfer-Cohen, 1977; Gilead & Bar-Yosef, 1993). When a technological analysis is applied, it is shown that management blanks, such as the thick and cortical asymmetrical debitage, occur mostly on blades (Davidzon & Goring-Morris, 2003; Hussain, 2015; Monigal, 2003; Parow-Souchon et al., 2021). At the moment, Qadesh Barnea 601 seems to be the only major southern Ahmarian site where blades (width 14 mm) are dominant within the assemblage (Gilead & Bar-Yosef, 1993).

Monigal (2003) shows that in Boker A bladelet cores are frequent, in addition to blade-bladelets cores. They also show a similar reduction sequence to blades-bladelets cores, only they are executed on purposely small raw material pieces. Such disassociation is rarely found in the other presented southern Ahmarian sites, where bladelets are predominant despite the use of a mostly single *chaîne opératoire*.

The reasons for such bladelet explosion during the Ahmarian, and in general for the EUP, are often linked with increased mobility and efficiency in raw material exploitation driven by the use of smaller nodules or less reliance on big, good quality raw material nodules (Bon, 2005; Kadowaki et al., 2021). Indeed, the southern Ahmarian shows a model of land use linked with highly mobile groups repeatedly visiting favourable locales where different resources (knappable material, food and water) were plentiful (Bar-Yosef & Belfer-Cohen, 1977; Davidzon & Goring-Morris, 2003; Gilead & Bar-Yosef, 1993; Kadowaki et al., 2015; Parow-Souchon et al., 2021; Phillips, 1988). Such focus on unidirectional, slender products is directly connected to the available chert sources, which mostly display a narrow edge. Nevertheless, as shown by this analysis, even when a broader volume was attainable, the knapper still preferred to parcel it in narrow volumes.

In contrast, the northern Ahmarian is mostly characterised by blade production from bidirectional, parallel-framed cores. In Kebara units IV and III, Ksar Akil levels XX/XIX–XIV, Üçağızlı layers C–B and Manot Cave area C unit 7, there is the same focus on blades obtained from bidirectional cores, and the flaking surface is still positioned on a narrow, longitudinal face (Abulafia et al., 2021; Bar-Yosef & Belfer-Cohen, 2019; Bergman, 1988; Kuhn et al., 2009; Ohnuma, 1988). Blades are parallel-sided and do not show the convergence found on blades in the south. Also, different from in the south, the main blank for creating convexities are bifacial crested blades (Ohnuma, 1988). Nevertheless, the core striking platforms are plain, and the overhang removal is thorough as in the southern Ahmarian, resulting in thin, small platforms. The higher frequency of blades does not seem to be an accident of antiquated excavation practices because Üçağızlı and Manot have been excavated with modern techniques (Abulafia et al., 2021; Kuhn, 2004). It has been noticed that, at least in Üçağızlı, the increase in bidirectional blade cores occurs with a shift in raw material procurement, as better quality raw material was imported from a more distant source. Thus, the bidirectional modality would have been a more efficient way of extracting blanks than the previous single platform cores (Kuhn, 2004; Kuhn et al., 2009). Tostevin (2013) observes that in Kebara the bidirectional modality applies most often in the first phases of the knapping, supporting the hypothesis that bidirectional knapping is reserved to obtain the longest possible blanks. The most interesting data comes from Manot: while the frequency for blade cores here is similar between bidirectional and unidirectional modalities, bladelet cores are only unidirectional and largely convergent (Abulafia et al., 2021). It is stressed that bladelet cores do not share a similar configuration with southern narrow-fronted cores, even though the only twisted elements cited are bladelets associated with pyramidal cores, which are reminiscent of the *débordant* elements in the south.

A peculiar case is represented by Mughr El-Hamamah, whose layer B, dated around 39–45 ka cal BP, probably represents several short-lived campsites sealed

by the historical age layer A (Shea et al., 2019). The prismatic cores are mostly similar to the sur tranche cores and produce mostly blades, but most of the cores are exploited through bipolar technology, classifying themselves among the scaled pieces. In addition, there are Levallois cores, some of them exhibiting a double patina and thus probably recycled (Shea et al., 2019, p. 5). The main negative pattern is bidirectional, not surprisingly due to the high frequency of bipolar cores. The focus seems to be on obtaining parallel blades and bladelets, with very few twisted elements. The knapping concepts employed on-site, despite not being dramatically different from the Ahmarian, are sufficiently unique to be recognised as a departure from it (Shea et al., 2019).

Typology

Contrary to most lithic points of earlier and later Palaeolithic phases, the el-Wad points show large variability not only in their metric dimensions but also in their overall shape and the retouch applied to them. This makes it difficult but crucial to investigate and compare every mentioned aspect to find a plausible explanation for their purpose. The comparison of metric dimensions of both simple blades/bladelets and el-Wad points shows that there are significant similarities regarding the width ($p > 0.05$; Fig. 12B), but that el-Wad points are both more elongated and longer than simple blades and bladelets. Although the width of the el-Wad points may have been reduced by retouch, the difference in median elongation between them and the simple blanks is too big to hypothesise that a reduction of the width through retouch affected the length/width ratio to such an extent. This hints that mostly large and elongated blanks underwent modification and that the rest of the central simple blades and bladelets were generally left unmodified. Although generally large and elongated dimensions were preferred, there is still some variation in the overall length and elongation (Table 12). On the other hand, a higher variability can be observed for the simple blank width, while the el-Wad points are concentrated between 10.2 and 13.3 mm (Table 12). Therefore, it can be stated that the preferred blank sizes are small blades and big bladelets, which, given their average length compared to those of simple blades and bladelets (Fig. 12A), mostly stem from the early reduction phases (Fig. 13: stage 2).

In addition to the shape-defining factors discussed above, symmetry has also been highlighted as an important attribute in the blank selection process (Davidzon & Goring-Morris, 2003). Its importance may also be reflected by the application of retouch on some el-Wad points. While there are no clear patterns visible regarding the location and type of retouch, in some cases it seems to fulfil a shaping purpose. This has been observed for the el-Wad points of Ksar Akil (Bergman, 1981) and also appears to some extent within the assemblage of Al-Ansab 1. Two examples (Fig. 9a, f) stand out where extensive retouch was presumably applied to provide symmetry. This may also explain the variety of retouch combinations as a result of individually reshaping some of the laminar blanks into the preferred final product. It

has to be noted though that not all points fit a concept of symmetry; some are asymmetrical (Fig. 9d, e). Possible reasons for this may be that they are either unfinished products or symmetry was not essential for this individual point.

The possibility of lateral hafting concerning el-Wad points has recently been raised and seems to be connected to the overall elongation and narrow shape of the points compared to those from the preceding Initial Upper Palaeolithic (Yaroshevich et al., 2021). If this is indeed the case, and the increase in the length of the sharp edge is seen as a way to increase the weapon's efficiency (Yaroshevich et al., 2021), a lateral hafting regarding the el-Wad points of Al-Ansab 1 seems very likely. Not only do 14 artefacts bear a continuous retouch along one dorsal edge, but they are on average also one of the longest el-Wad point assemblages of the southern Ahmarian (in comparison to the sites investigated by Kadowaki et al., 2015).

However, the variability in size among el-Wad points is undeniable, and even though there are also small points present, they show different retouch patterns. While most of the points are retouched on the dorsal face, with the right edge being favoured (Fig. 8), only the smallest el-Wad points show inverse retouch. This indicates that size may be an important factor for the decision between dorsal and ventral retouch and may also point to a different use or hafting purpose. To confirm this hypothesis, a comparison of use-wear between both inverse and obverse retouched el-Wad points is necessary. The strict distinction between inverse and obverse retouch also stands out compared to other sites of the southern Ahmarian (Tor Sadaf & EHLPP1) where, contrary to the site of Al-Ansab 1, el-Wad points with alternating retouch are present (Coinman, 2003). However, the lack of quantifiable data regarding other Ahmarian sites limits the value of this observation.

The purpose of el-Wad points has been a topic of interest for quite some time. While they are typically referred to as projectile points (Newcomer & Bergman, 1983; Shea, 2006; Sisk & Shea, 2011), a more versatile use also involving cutting and butchering procedures has been suggested (Eren & Kuhn, 2019; Parow-Souchon et al., 2021). The limited research that has been conducted on use-wear regarding el-Wad points focuses mainly on macroscopic impact fractures and provides indications of such fractures being present on el-Wad points of different Ahmarian assemblages, including the sites of Ksar Akil and Üçağızlı (Bergman, 1981; Eren & Kuhn, 2019; Newcomer & Bergman, 1983). To ensure an accurate recognition and analysis of use-wear, extensive training, as well as a large set of experimental tools, is essential (Rots & Plisson, 2014). Since neither of these was available, no proper use-wear analysis has been conducted on the assemblage of Al-Ansab 1. Nevertheless, at least one of the el-Wad points under investigation showed a burination scar, which might be linked to a possible impact fracture, but it will need further investigation to be confirmed (Fig. 9h). It has been stated before that a low frequency in diagnostic impact fracture (DIF) might be a result of lateral hafting (Yaroshevich et al., 2021). The tips of laterally hafted points or blades are less vulnerable to impact and therefore lead to fewer DIFs (Yaroshevich et al., 2013). Hence, we assume that most el-Wad points of the Ansab assemblage were non-tip lateral hafted elements.

Conclusion

The raw data coming from rich, recently excavated sites like Al-Ansab 1 is pivotal for advancing knowledge of a technocomplex. We have explored and updated the relationship between the southern Ahmarian technology and its cultural marker: the el-Wad point. The technology at Al-Ansab 1 revolves around the obtention of bladelets (blades smaller than 12 mm wide) from unidirectional platform cores. There is no correlation between core original size and blank size, i.e. bladelets seem to have been sought-after blanks since the start of the reduction. Conversely, blades are still an important part of the reduction, but mostly for shaping roles creating the perfect volumes for the bladelets. The differentiated production is likely to be intentional because the management items are frequently turned into heavier-duty tools, like burins or scrapers (Davidzon & Goring-Morris, 2003; Hussain, 2015; Monigal, 2003; Parow-Souchon et al., 2021). Nevertheless, the emphasis on Ahmarian knapping products is often placed on the slender, regular, symmetrical and straight blades and bladelets coming from the central volumes of cores and highlighted by the management negatives. El-Wad points are primarily made on this type of blank (Belfer-Cohen & Goring-Morris, 2008). As projectile points and cutting knives, these were probably the main part of the mobile personal toolkit and were therefore consequential to the high degree of mobility and exploitation of the Ahmarian landscape.

In Al-Ansab 1, morpho-technological characteristics, often referred to as el-Wad points and Ahmarian lithic production, are mostly tied to bladelets. A thorough review of the existing literature shows that most of the southern Ahmarian assemblages follow this trend, even if a formal division between bladelet and blade roles is not applied by the original authors. When looking at Ansab's el-Wad points specifically, we notice that they sit mostly at the threshold between blades and bladelets, despite being skewed towards the bladelets. Retouch patterns are consistent mostly with edge adjustment for hafting but, in some cases, it could also indicate a higher degree of shaping, especially towards the tip. Thus, we argue that retouch mostly concerned blanks obtained in the first stages of the core reduction. Nevertheless, reduction continued and several of the cores are extremely reduced, as can be observed in other Ahmarian sites (e.g. Nahal Nizzana XIII (Davidzon & Goring-Morris, 2003)). In other sites, the knappers intentionally selected small nodules for obtaining bladelets (Monigal, 2003). Interestingly, in Al-Ansab 1, bladelets are the only blanks that bear an inverse retouch, maybe denoting a differential treatment for the smallest of the retouched implements. The obtention of progressively smaller and more regular implements is a constant in the debate over the adoption of more and more sophisticated projectile technologies (Sano et al., 2019). The dichotomy is often between an implement that is technologically curated against one that is typologically curated (Belfer-Cohen & Goring-Morris, 2008). Studies of this nature still need to be widely applied to Levantine Upper Palaeolithic assemblages, but it seems that the southern Ahmarian already represents a full shift towards small projectile technology.

Acknowledgements We thank the Department of Antiquities (Amman/Jordan) for granting the excavation permits and Professor Maysoon Al Nahar from the University of Jordan, Amman, for supporting logistics and student participation. We thank the two anonymous reviewers who have contributed to improving the paper.

Author Contribution Conceptualisation: J.G., M.S., J.R. Methodology: J.G., M.S., J.R. Formal analysis: J.G., M.S. Investigation: J.G. (technology), M.S. (typology), J.R. (archaeological excavation). Resources: J.R. Data curation: J.G., M.S., J.R. Writing—original draft: J.G., M.S., J.R. Writing—review and editing: J.G., M.S., J.R. Visualisation: J.G., M.S. Supervision: J.R. Funding acquisition: J.R.

Funding Open Access funding enabled and organized by Projekt DEAL. J.G.'s Ph.D. research and research et al.-Ansab 1 was funded by the Deutsche Forschungsgemeinschaft (DFG, German Research Foundation) – Projektnummer 57444011 – SFB 806.

Data Availability The datasets generated during and/or analysed during the current study are either included in the published article or available in the CRC806 database repository, www.crc806db.uni-koeln.de (Gennai, J., Schemmel, M. (2022): Data on flakes, blades, cores, and el-Wad points from Al-Ansab 1 AH1. CRC806-Database, https://doi.org/10.5880/SFB806.80).

Declarations

Conflict of Interest The authors declare no competing interests.

References

Abulafia, T., Goder-Goldberger, M., Berna, F., Barzilai, O., & Marder, O. (2021). A technotypological analysis of the Ahmarian and Levantine Aurignacian assemblages from Manot Cave (area C) and the interrelation with site formation processes. *Journal of Human Evolution, 160*, 102707. https://doi.org/10.1016/j.jhevol.2019.102707

Alex, B., Barzilai, O., Hershkovitz, I., Marder, O., Berna, F., Caracuta, V., et al. (2017). Radiocarbon chronology of Manot Cave, Israel and Upper Paleolithic dispersals. *Science Advances, 3*(11), e1701450. https://doi.org/10.1126/sciadv.1701450

Andrefsky, W. (2005). *Lithics: macroscopic approaches to analysis* (2nd ed.). Cambridge: Cambridge University Press.

Audouze, F., & Karlin, C. (2017). La chaîne opératoire a 70 ans : Qu'en ont fait les préhistoriens français. *Journal of Lithic Studies, 4*(2), 5–73. https://doi.org/10.2218/jls.v4i2.2539

Bar-Yosef, O., & Belfer-Cohen, A. (1977). The Lagaman Industry. In O. Bar-Yosef & J. L. Phillips (Eds.), *Prehistoric investigations in Gebel Maghara, Northern Sinai* (Qedem., Vols 1–7, pp. 42–85).

Bar-Yosef, O., & Belfer-Cohen, A. (2019). The Upper Paleolithic Industries of Kebara Cave. In L. Meignen & O. Bar-Yosef (Eds.), *Kebara Cave, Mt. Carmel, Israel: the Middle and Upper Paleolithic archaeology: part 2* (pp. 309–401). Harvard University: Peabody Museum of Archaeology and Ethnology.

Bataille, G., Tafelmaier, Y., & Weniger, G.-C. (2018). Living on the edge – a comparative approach for studying the beginning of the Aurignacian. *Quaternary International, 474*, 3–29. https://doi.org/10.1016/j.quaint.2018.03.024

Belfer-Cohen, A., & Goring-Morris, N. (2009). The shift from the Middle Palaeolithic to the Upper Palaeolithic: Levantine perspectives. In Marta Camps & C. C. Szmidt (Eds.), *The Mediterranean from 50 000 to 25 000 BP:Turning Points and New Directions* (pp. 89–100). Oxford: Oxbow Books.

Belfer-Cohen, A., & Goring-Morris, N. (2008). Why microliths? Microlithization in the Levant. *Archeological Papers of the American Anthropological Association, 12*(1), 57–68. https://doi.org/10.1525/ap3a.2002.12.1.57

Bergman, C. A., & Stringer, C. B. (1989). Fifty years after: Egbert, an early Upper Palaeolithic juvenile from Ksar Akil, Lebanon. *Paléorient*, *15*(2), 99–111. https://doi.org/10.3406/paleo.1989.4512

Bergman, C. A. (1981). Point types in the Upper Palaeolithic sequence at Ksar Akil, Lebanon. In J. Cauvin & P. Sanlaville (Eds.), *Préhistoire du Levant: chronologie et organisation de l'espace depuis les origines jusqu'au VIe millénaire: Lyon, Maison de l'Orient méditerranéen, 10–14 juin 1980: [colloque organisé par Jacques Cauvin et Paul Sanlaville]* (pp. 319–330). Paris: Editions du Centre national de la recherche scientifique.

Bergman, C. A. (1988). Ksar Akil and the upper palaeolithic of the levant. *Paléorient*, *14*(2,), 201–210.

Bertrams, M., Protze, J., Löhrer, R., Schyle, D., Richter, J., Hilgers, A., et al. (2012). Multiple environmental change at the time of the Modern Human passage through the Middle East: First results from geoarcheological investigations on Upper Pleistocene sediments in the Wadi Sabra (Jordan). *Quaternary International, 274*, 55–72. https://doi.org/10.1016/j.quaint.2012.02.047

Boaretto, E., Hernandez, M., Goder-Goldberger, M., Aldeias, V., Regev, L., Caracuta, V., et al. (2021). The absolute chronology of Boker Tachtit (Israel) and implications for the Middle to Upper Paleolithic transition in the Levant. *Proceedings of the National Academy of Sciences, 118*(25), e2014657118. https://doi.org/10.1073/pnas.2014657118

Bon, F. (2002). *L' Aurignacien entre mer et océan: Réflexion sur l'unité des phases anciennes de l'Aurignacien dans le sud le la France*. Soc. Préhistorique Française.

Bon, F. (2005). Little big tool enquête autour du succès de la lamelle. In F. Le Brun-Ricalens (Ed.), *Actes du XIVème congrès UISPP, Université de Liège, Belgique, 2 - 8 septembre 2001: session 6, Paléolithique supérieur ; section 6 - Upper Palaeolithic. Productions lamellaires attribuées à l'Aurignacien : Chaînes opératoires et perspectives technoculturelles* (pp. 479–484). Luxèmbourg: Musée National d'Histoire et d'Art.

Bosch, M. D., Mannino, M. A., Prendergast, A. L., O'Connell, T. C., Demarchi, B., Taylor, S. M., et al. (2015). New chronology for Ksâr 'Akil (Lebanon) supports Levantine route of modern human dispersal into Europe. *Proceedings of the National Academy of Sciences, 112*(25), 7683–7688. https://doi.org/10.1073/pnas.1501529112

Bronk Ramsey, C. (2009). Bayesian analysis of radiocarbon dates. *Radiocarbon, 51*(1), 337–360. https://doi.org/10.1017/S0033822200033865

Chiotti, L., & Cretin, C. (2011). Les mises en forme de grattoirs carénés/ nucléus de l'aurignacien ancien de l'abri Castanet (Sergeac, Dordogne). *PALEO Revue D'archéologie Préhistorique, 22*, 69–84.

Coinman, N. R. (2005). Subsistence and technology in the Late Levantine Upper Paleolithic. *Mitekufat Haeven: Journal of the Israel Prehistoric Society, 35*, 159–177.

Coinman, N. R. (2003). The Upper Palaeolithic of Jordan: new data from the Wadi al-Hasa. In N. Goring-Morris & A. Belfer-Cohen (Eds.), *More than meets the eye: studies on Upper Palaeolithic diversity in the Near East*. Oxbow Books. https://doi.org/10.2307/j.ctvh1dwcq

Conard, N. J., Soressi, M., Parkington, J. E., Wurz, S., & Yates, R. (2004). A unified lithic taxonomy based on patterns of core reduction. *The South African Archaeological Bulletin, 59*(179), 13–17. https://doi.org/10.2307/3889318

Davidzon, A., & Goring-Morris, N. (2003). Sealed in stone: The Upper Palaeolithic Early Ahmarian knapping method in the light of refitting studies at Nahal Nizzana XIII, Western Negev, Israel. *Journal of the Israel Prehistoric Society, 33*, 75–205.

Douka, K. (2013). Exploring "the great wilderness of prehistory": The chronology of the Middle to the Upper Paleolithic transition in the Northern Levant. *Mitteilungen Der Gesellschaft Für Urgeschichte, 22*, 11–39.

Douka, K., Bergman, C. A., Hedges, R. E. M., Wesselingh, F. P., & Higham, T. F. G. (2013). Chronology of Ksar Akil (Lebanon) and implications for the colonization of Europe by anatomically modern humans. *PLoS ONE, 8*(9), e72931. https://doi.org/10.1371/journal.pone.0072931

Douka, K., Higham, T. F. G., & Bergman, C. A. (2015). Statistical and archaeological errors invalidate the proposed chronology for the site of Ksar Akil. *Proceedings of the National Academy of Sciences, 112*(51), E7034–E7034. https://doi.org/10.1073/pnas.1519746112

Driscoll, K., & García-Rojas, M. (2014). Their lips are sealed: Identifying hard stone, soft stone, and antler hammer direct percussion in Palaeolithic prismatic blade production. *Journal of Archaeological Science, 47*, 134–141. https://doi.org/10.1016/j.jas.2014.04.008

Eren, E., & Kuhn, S. L. (2019). Morphological and functional variation in points from the Ahmarian layers at Üçağızlı Cave, Turkey. *Eurasian Journal of Anthropology, 10*(1), 1–19.

Falcucci, A., & Peresani, M. (2018). Protoaurignacian core reduction procedures: Blade and bladelet technologies at Fumane Cave. *Lithic Technology, 43*(2), 125–140. https://doi.org/10.1080/01977261.2018.1439681

Falcucci, A., Conard, N. J., & Peresani, M. (2017). A critical assessment of the Protoaurignacian lithic technology at Fumane Cave and its implications for the definition of the earliest Aurignacian. *PLoS ONE, 12*(12), e0189241. https://doi.org/10.1371/journal.pone.0189241

Falcucci, A., Conard, N. J., & Peresani, M. (2020). Breaking through the Aquitaine frame: A re-evaluation on the significance of regional variants during the Aurignacian as seen from a key record in southern Europe. *Journal of Anthropological Sciences, 98*, 42.

Fox, J. R. (2003). The Tor Sadaf lithic assemblages: a technological study of the Early Upper Palaeolithic in the Wadi al-Hasa. In N. Goring-Morris & A. Belfer-Cohen (Eds.), *978-1-78570-917-3 978-1-78570-914-2* (pp. 80–94).

Garrod, D. (1957). Notes sur le paléolithique supérieur du moyen orient. *Bulletin De La Société Préhistorique De France, 54*(7), 439–446. https://doi.org/10.3406/bspf.1957.7854

Gennai, J. (2021). *Back to the lithics: technological comparison of early Upper Palaeolithic assemblages from Al-Ansab/Jordan, Românești-Dumbrăviţa/Romania and Fumane/Italy* (Doctoral thesis). Universität zu Köln Philosophische Fakultät Institut für Ur- und Frühgeschichte, Köln. Retrieved from http://kups.ub.uni-koeln.de/id/eprint/53384. Accessed 11 April 2022.

Gilead, I. (1991). The upper Paleolithic period in the Levant. *Journal of World Prehistory, 5*(2), 105–154. https://doi.org/10.1007/BF00974677

Gilead, I., & Bar-Yosef, O. (1993). Early upper Paleolithic sites in the Qadesh Barnea Area, NE Sinai. *Journal of Field Archaeology*, *20*(3), 265–280.

Gilead, I. (1981). Upper Palaeolithic tool assemblages from the Negev and Sinai. In J. Cauvin (Ed.), *Préhistoire du Levant. Chronologie et organisation de l'espace depuis les origines jusq'au VIe millénaire.* (Vol. 598, pp. 5581–5581). Paris: Ed. du CNRS. https://pubs.acs.org/doi/abs/10.1021/ja01553a083. Accessed 11 April 2022.

Goring-Morris, N., & Belfer-Cohen, A. (2018). The Ahmarian in the context of the Earlier Upper Palaeolithic in the Near East. In Y. Nishiaki & T. Akazawa (Eds.), *The Middle and Upper Paleolithic archeology of the Levant and beyond* (pp. 87–104). Singapore: Springer Singapore. https://doi.org/10.1007/978-981-10-6826-3_7

Hublin, J.-J. (2015). The modern human colonization of western Eurasia: When and where? *Quaternary Science Reviews, 118*, 194–210. https://doi.org/10.1016/j.quascirev.2014.08.011

Hussain, S. T. (2015). Betwixt seriality and sortiment: rethinking early Ahmarian blade technology in Al-Ansab 1. In D. Schyle & J. Richter (Eds.), *Pleistocene archaeology of the Petra area in Jordan* (pp. 131–147). Rahden/Westf: Leidorf.

Inizan, M.-L., Reduron-Ballinger, M., Roche, H., Tixier, J., & Féblot-Augustins, J. (Eds.). (1999). *Technology and terminology of knapped stone: followed by a multilingual vocabulary – Arabic, English, French, German,Greek, Italian, Portuguese, Spanish*. Nanterre: CREP.

Kadowaki, S., Omori, T., & Nishiaki, Y. (2015). Variability in Early Ahmarian lithic technology and its implications for the model of a Levantine origin of the Protoaurignacian. *Journal of Human Evolution, 82*, 67–87. https://doi.org/10.1016/j.jhevol.2015.02.017

Kadowaki, S., Suga, E., & Henry, D. O. (2021). Frequency and production technology of bladelets in Late Middle Paleolithic, Initial Upper Paleolithic, and Early Upper Paleolithic (Ahmarian) assemblages in Jebel Qalkha, Southern Jordan. *Quaternary International, 596*, 4–21. https://doi.org/10.1016/j.quaint.2021.03.012

Klasen, N., Hilgers, A., Schmidt, C., Bertrams, M., Schyle, D., Lehmkuhl, F., et al. (2013). Optical dating of sediments in Wadi Sabra (SW Jordan). *Quaternary Geochronology, 18*, 9–16. https://doi.org/10.1016/j.quageo.2013.08.002

Kuhn, S. L. (2004). From Initial Upper Paleolithic to Ahmarian at Üçağızlı cave, Turkey. *Anthropologie, XLI*(3), 249–262.

Kuhn, S. L., Stiner, M. C., Güleç, E., Özer, I., Yılmaz, H., Baykara, I., et al. (2009). The early Upper Paleolithic occupations at Üçağızlı Cave (Hatay, Turkey). *Journal of Human Evolution, 56*(2), 87–113. https://doi.org/10.1016/j.jhevol.2008.07.014

Laplace, G. (1966). *Recherches sur l'origine et l'évolution des complexes leptolithiques*. École Française de Rome.

Le Brun-Ricalens, F., Bordes, J.-G., & Eizenberg, L. (2009). A crossed-glance between southern European and Middle-Near Eastern Early Upper Palaeolithic lithic technocomplexes. Existing models, new perspectives. In M. Camps & C. C. Szmidt (Eds.), *The Mediterranean from 50 000 to 25 000 BP: Turning Points and New Directions* (Oxbow Books., pp. 11–33). Oxford.

Marks, A. E. (Ed.). (1976). *Prehistory and paleoenvironments in the central Negev, Israel*. SMU Press.

Monigal, K. (2003). Technology, economy, and mobility at the beginning of the Levantine Upper Palaeolithic. In N. Goring-Morris & A. Belfer-Cohen (Eds.), *More than meets the eye: studies on Upper*

Palaeolithic Diversity in the Near East (pp. 118–133). Oxford : Oakville, CT: Oxbow Books ; David Brown Book Co. https://doi.org/10.2307/j.ctvh1dwcq

Neuville, R. (1934). Le Préhistorique de Palestine. *Revue Biblique, 43*(2), 237–259.

Newcomer, M. H., & Bergman, C. A. (1983). Flint arrowhead breakage: Examples from Ksar Akil, Lebanon. *Journal of Field Archaeology, 10*, 238–243.

Normand, C., & Turq, A. (2005). L'Aurignacien de la Grotte d'Isturitz (France); la production lamellaire dans la séquence de la salle de Saint-Martin. In F. Le Brun-Ricalens (Ed.), *Productions lamellaires attribuées à l'Aurignacien: actes du XIVe congrès de l'UISPP, Université de Liège, 2–8 septembre 2001, section 6, symposium C6.7* (pp. 375–392). Luxembourg: Musée National d'Histoire et d'Art.

Ohnuma, K. (1988). *Ksar Akil, Lebanon. Vol. 3: A technological study of the earlier upper palaeolithic levels of Ksar Akil, levels 25 - 14* (Vol. 3). Oxford: BAR.

Parow-Souchon, H. (2020). *The Wadi Sabra (Jordan): A contextual approach to the palaeolithic landscape: A CRC 806 monograph*. Verlag Marie Leidorf GmbH.

Parow-Souchon, H., Hussain, S. T., & Richter, J. (2021). Early Ahmarian Lithic Techno-Economy and Mobility at Al-Ansab 1, Wadi Sabra, Southern Jordan. *Journal of the Israel Prehistoric Society, 51*, 6–64.

Patil, I. (2021). Visualizations with statistical details: the 'ggstatsplot' approach. *Journal of Open Source Software*, *6*(61), 3167. https://doi.org/10.21105/joss.03167

Pelegrin, J. (2000). Les techniques de débitage laminaire au Tardiglaciaire: critères de diagnose et quelques réflexions. In B. Valentin, P. Bodu, & M. Christensen (Eds.), *L'Europe centrale et septentrionale au Tardiglaciaire : confrontation des modèles régionaux de peuplement. Actes de la table-ronde internationale de Nemours, 14–16 mai 1997* (Vol. 7, pp. 73–86). Nemours: Association pour la promotion de la recherche archéologique en Ile-de-France.

Pelegrin, J. (2011). Sur les débitages laminaires du Paléolithique Supérieur. In F. Delpech & J. Jaubert (Eds.), *François bordes et la préhistoire colloque international françois bordes, bordeaux, 22–24 avril 2009* (pp. 141–152). Ed. du CHTS.

Phillips, J. L. (1988). The Upper Paleolithic of the Wadi Feiran, Southern Sinai. *Paléorient*, *14*(2), 183–200. https://doi.org/10.3406/paleo.1988.4467

Phillips, J. L. (1994). The Upper Palaeolithic chronology of the Levant and the Nile Valley. In O. Bar-Yosef & R. S. Kra (Eds.), *Late Quaternary chronology and palaeoclimates of the Eastern Mediterranean* (pp. 169–176). Tucson, Ariz., USA : Cambridge, Mass., USA: RADIOCARBON ; American School of Prehistoric Research. Accessed 13 July 2022

Porraz, G., Simon, P., & Pasquini, A. (2010). Identité technique et comportements économiques des groupes proto-aurignaciens à la grotte de l'Observatoire (principauté de Monaco). *Gallia Préhistoire, 52*(1), 33–59. https://doi.org/10.3406/galip.2010.2470

R Core Team. (2020). *R: A language and environment for statistical computing*. R Foundation for Statistical Computing, Vienna, Austria. URL https://www.R-project.org/. Accessed 24 April 2020

Rebollo, N. R., Weiner, S., Brock, F., Meignen, L., Goldberg, P., Belfer-Cohen, A., et al. (2011). New radiocarbon dating of the transition from the Middle to the Upper Paleolithic in Kebara Cave, Israel. *Journal of Archaeological Science, 38*(9), 2424–2433. https://doi.org/10.1016/j.jas.2011.05.010

Reimer, P. J., Austin, W. E. N., Bard, E., Bayliss, A., Blackwell, P. G., Bronk Ramsey, C., et al. (2020). The IntCal20 Northern Hemisphere Radiocarbon Age Calibration Curve (0–55 cal kBP). *Radiocarbon, 62*(4), 725–757. https://doi.org/10.1017/RDC.2020.41

Richter, J., Litt, T., Lehmkuhl, F., Hense, A., Hauck, T. C., Leder, D. F., et al. (2020). Al-Ansab and the Dead Sea: Mid-MIS 3 archaeology and environment of the early Ahmarian population of the Levantine corridor. *PLoS ONE, 15*(10), e0239968. https://doi.org/10.1371/journal.pone.0239968

Rots, V., & Plisson, H. (2014). Projectiles and the abuse of the use-wear method in a search for impact. *Journal of Archaeological Science, 48*, 154–165. https://doi.org/10.1016/j.jas.2013.10.027

Roussel, M., Bourguignon, L., & Soressi, M. (2009). Identification par l'expérimentation de la percussion au percuteur de calcaire au Paléolithique moyen : Le cas du façonnage des racloirs bifaciaux Quina de Chez Pinaud (Jonzac, Charente-Maritime). *Bulletin De La Société Préhistorique Française, 106*(2), 219–238. https://doi.org/10.3406/bspf.2009.13846

Sano, K., Arrighi, S., Stani, C., Aureli, D., Boschin, F., Fiore, I., et al. (2019). The earliest evidence for mechanically delivered projectile weapons in Europe. *Nature Ecology & Evolution, 3*(10), 1409–1414. https://doi.org/10.1038/s41559-019-0990-3

Sauer, F., & Schoenenberg, J. (2021). Gazelle hunting strategies in the Early Ahmarian: close-range visuospatial characteristics of site locations indicate spatially focused hunting strategies on Gazella sp. during the Early Ahmarian. *Journal of Paleolithic Archaeology*, *4*(3), 22. https://doi.org/10.1007/s41982-021-00090-9

Scerri, E. M. L., Gravina, B., Blinkhorn, J., & Delagnes, A. (2016). Can lithic attribute analyses identify discrete reduction trajectories? A quantitative study using refitted lithic sets. *Journal of Archaeological Method and Theory, 23*(2), 669–691. https://doi.org/10.1007/s10816-015-9255-x

Schlanger, N. (2004). « Suivre les gestes, éclat par éclat » – la chaîne opératoire d'André Leroi-Gourhan. In F. Audouze & N. Schlanger (Eds.), *Autour de l'homme : contexte et actualité d'André Leroi-Gourhan* (pp. 127–147). Antibes: AP-DCA.

Schoenenberg, J., & Sauer, F. (2022). Intra-site structure of the Early Ahmarian site of Al-Ansab 1, AH 1 (Jordan). *Journal of Paleolithic Archaeology, 5*(1), 2. https://doi.org/10.1007/s41982-021-00103-7

Schyle, D. (2015). The Ahmarian site of al-Ansab 1. In D. Schyle & J. Richter (Eds.), *Pleistocene archaeology of the Petra area in Jordan* (pp. 91–130). Rahden/Westf: Leidorf.

Shea, J. J. (2006). The origins of lithic projectile point technology: Evidence from Africa, the Levant, and Europe. *Journal of Archaeological Science, 33*(6), 823–846. https://doi.org/10.1016/j.jas.2005.10.015

Shea, J. J. (2013). *Stone tools in the Paleolithic and Neolithic Near East: A guide*. Cambridge University Press. https://doi.org/10.1017/CBO9781139026314

Shea, J. J., Stutz, A. J., & Nilsson-Stutz, L. (2019). An Early Upper Palaeolithic stone tool assemblage from Mughr El-Hamamah, Jordan: An interim report. *Journal of Field Archaeology, 44*(7), 420–439. https://doi.org/10.1080/00934690.2019.1655519

Sisk, M. L., & Shea, J. J. (2011). The African origin of complex projectile technology: An analysis using tip cross-sectional area and perimeter. *International Journal of Evolutionary Biology, 2011*, 1–8. https://doi.org/10.4061/2011/968012

Slimak, L., Pesesse, D., & Giraud, Y. (2002). La grotte Mandrin et les premières occupations du Paléolithique supérieur en Occitanie orientale. *Espacio Tiempo y Forma. Serie I, Prehistoria y Arqueología*, *1*(15), 237–259. https://doi.org/10.5944/etfi.15.2002.4746

Soressi, M., & Geneste, J.-M. (2011). The history and efficacy of the chaîne opératoire approach to lithic analysis: studying techniques to reveal past societies in an evolutionary perspective. *PaleoAnthropology*, (Special Issue: Reduction Sequence, Chaîne Opératoire, and Other Methods: The Epistemologies of Different Approaches to Lithic Analysis), 334–350.

Teyssandier, N., Bon, F., & Bordes, J.-G. (2010). Within projectile range: Some thoughts on the appearance of the Aurignacian in Europe. *Journal of Anthropological Research, 66*(2), 209–229. https://doi.org/10.3998/jar.0521004.0066.203

Tixier, J. (1963). *Typologie de l'épipaléolithique du Maghreb* (Vols 1-2). Paris: Arts et Métiers Graphiques.

Tostevin, G. B. (2013). *Seeing lithics: a middle-range theory for testing for cultural transmission in the Pleistocene*. Oxford: Oakville, CT : Oxbow Books.

Weinstein, J. M. (1984). Radiocarbon dating in the Southern Levant. *Radiocarbon, 26*(3), 297–366. https://doi.org/10.1017/S0033822200006731

Yaroshevich, A., Nadel, D., & Tsatskin, A. (2013). Composite projectiles and hafting technologies at Ohalo II (23 ka, Israel): Analyses of impact fractures, morphometric characteristics and adhesive remains on microlithic tools. *Journal of Archaeological Science, 40*(11), 4009–4023. https://doi.org/10.1016/j.jas.2013.05.017

Yaroshevich, A., Kaufman, D., & Marks, A. (2021). Weapons in transition: Reappraisal of the origin of complex projectiles in the Levant based on the Boker Tachtit stratigraphic sequence. *Journal of Archaeological Science, 131*, 105381. https://doi.org/10.1016/j.jas.2021.105381

Zilhão, J. (2013). Neandertal-modern human contact in Western Eurasia: issues of dating, taxonomy, and cultural associations. In T. Akazawa, Y. Nishiaki, & K. Aoki (Eds.), *Dynamics of learning in Neanderthals and modern humans volume 1* (pp. 21–57). Tokyo: Springer Japan. https://doi.org/10.1007/978-4-431-54511-8_3

Authors and Affiliations

Jacopo Gennai[1] · Marcel Schemmel[1] · Jürgen Richter[1]

[1] Institute of Prehistoric Archaeology, University of Cologne, Weyertal, 125, 50931 Cologne, Germany